^{13}C NMR and Fluorescence Analysis of Tryptophan Dynamics in Wild-Type and Two Single-Trp Variants of *Escherichia coli* Thioredoxin

Marvin D. Kemple,[‡] Peng Yuan,[‡] Kenneth E. Nollet,[§] James A. Fuchs,[¶] Norberto Silva,[§] and Franklyn G. Prendergast*[§]

[‡]Department of Physics, Indiana University-Purdue University Indianapolis, Indianapolis, Indiana 46202-3273, [§]Department of Biochemistry and Molecular Biology, Mayo Foundation, Rochester, Minnesota 55905, and [¶]Department of Biochemistry, College of Biological Sciences, University of Minnesota, St. Paul, Minnesota 55108 USA

ABSTRACT The rotational motion of tryptophan side chains in oxidized and reduced wild-type (WT) *Escherichia coli* thioredoxin and in two single-tryptophan variants of *E. coli* thioredoxin was studied in solution in the temperature range 20–50°C from ^{13}C-NMR relaxation rate measurements at 75.4 and 125.7 MHz and at 20°C from steady-state and time-resolved trp fluorescence anisotropy measurements. Tryptophan enriched with ^{13}C at the δ_1 and ϵ_3 sites of the indole ring was incorporated into WT thioredoxin and into two single-trp mutants, W31F and W28F, in which trp-28 or trp-31 of WT thioredoxin was replaced, respectively, with phenylalanine. The NMR relaxation data were interpreted using the Lipari and Szabo "model-free" approach (G. Lipari and A. Szabo. 1982. *J. Amer. Chem. Soc.* 104:4546–4559) with trp steady-state anisotropy data included for the variants at 20°C. Values for the correlation time for the overall rotational motion (τ_m) from NMR of oxidized and reduced WT thioredoxin at 35°C agree well with those given by Stone et al. (Stone, M. J., K. Chandrasekhar, A. Holmgren, P. E. Wright, and H. J. Dyson. 1993. *Biochemistry.* 32:426–435) from ^{15}N NMR relaxation rates, and the dependence of τ_m on viscosity and temperature was in accord with the Stokes-Einstein relationship. Order parameters (S^2) near 1 were obtained for the trp side chains in the WT proteins even at 50°C. A slight increase in the amplitude of motion (decrease in S^2) of trp-31, which is near the protein surface, but not of trp-28, which is partially buried in the protein matrix, was observed in reduced relative to oxidized WT thioredoxin. For trp-28 in W31F, order parameters near 1 ($S^2 \geq 0.8$) at 20°C were found, whereas trp-31 in W28F yielded the smallest order parameters ($S^2 \sim 0.6$) of any of the cases. Analysis of time-resolved anisotropy decays in W28F and W31F yielded S^2 values in good agreement with NMR, but gave τ_m values about 60% smaller. Generally, values of τ_e, the effective correlation time for the internal motion, were ≤60 ps from NMR, whereas somewhat longer times were obtained from fluorescence. The ability of NMR and fluorescence techniques to detect sub-nanosecond motions in proteins reliably is examined.

INTRODUCTION

The existence of picosecond internal motions in peptides and proteins is predicted by computer simulations of molecular dynamics, and their presence can be shown directly through use of various experimental techniques such as fluorescence and NMR, and less directly from x-ray crystallography and neutron scattering data (McCammon and Harvey, 1987; Brooks et al., 1988). These motions are, however, difficult to quantify and questions remain regarding their amplitude and time scale. We are attempting to address some of these issues, particularly the precise and, we hope, accurate determination of motional parameters by using NMR and fluorescence measurements on ^{13}C-enriched tryptophan residues incorporated biosynthetically into proteins. With this approach the experiments can be conducted under nearly identical experimental conditions and in principle we expect that the results from fluorescence will corroborate those obtained from NMR and vice versa.

Thioredoxin (TRX), a relatively small (molecular weight 11,700), nearly spherical, and seemingly ubiquitous protein containing a disulfide bridge at its active site and functioning in thiol-disulfide interchange (Holmgren, 1985), is an interesting and appropriate choice for studies of trp dynamics. The thiol side chains of TRX participate in electron transfer reactions with the disulfides of other proteins such as thioredoxin reductase, ribonucleotide reductase, methionine sulfoxide reductase, and adenosine 3′-phosphate 5′-phosphosulfate reductase. Reduced TRX also apparently plays a structural role in the life cycle of phages M13, T4, and T7 (Holmgren, 1985, 1989). *E. coli* TRX contains 108 amino acid residues. Its active site is composed of cysteine

Received for publication 19 January 1994 and in final form 24 March 1994.

Address reprint requests to Marvin D. Kemple, Department of Physics, IUPUI, 402 North Blackford Street, Indianapolis, IN 46202-3273. Tel.: 317-274-6906; Fax: 317-274-2393; E-mail: mkemple@indyvax.iupui.edu.

Abbreviations used: COSY, correlated spectroscopy; CPMG, Carr Purcell Meiboom Gill; CSA, chemical shift anisotropy; DD, dipole-dipole; DEAE, diethylaminoethyl; DTNB, 5,5′-dithiobis-(2-nitrobenzoic acid); DTT, dithiothreitol; FT, Fourier transform; HMQC, heteronuclear multiple quantum filtered COSY; IPTG, isopropyl β-D-thioglucopyranoside; IUPUI, Indiana University-Purdue University Indianapolis; LW, linewidth; MD, molecular dynamics; NOE, steady-state nuclear Overhauser Effect; PAGE, polyacrylamide gel electrophoresis; TCEP, tris(2-carboxyethyl)phosphine; TRIS, tris(hydromethyl)aminomethane; SDS, sodium dodecyl sulfate; TRX, *E. coli* thioredoxin; TSP, sodium 3-(trimethylsilyl) propionate-2, 2, 3, 3-d_4; WT, wild-type; WT-TRX wild-type *E. coli* thioredoxin; W28F; single tryptophan variant of TRX with tryptophan-28 replaced by phenylalanine; W31F, single tryptophan variant of TRX with tryptophan-31 replaced by phenylalanine.

0006-3495/94/06/2111/16 $2.00

residues at positions 32 and 35, and it has two trp residues, one at position 28 and the other at position 31, whose fluorescence spectra have been characterized (Holmgren, 1972). X-ray (Holmgren et al., 1975; Katti et al., 1990) and NMR (Dyson et al., 1990) structural studies of TRX have shown that trp-31 lies on the surface of the protein comprising part of an hydrophobic patch that may be involved in substrate binding, and that trp-28 is partially buried in the protein matrix. Both trp residues are near the active site as can be seen from Fig. 1, a stick representation of the vicinity of the active site of oxidized TRX constructed from the x-ray coordinates. Potentially, differences in the internal dynamics of the two trp residues between the two oxidation states of TRX could be expected.

Because TRX is stable at temperatures up to 80°C (Reutimann et al., 1981; Holmgren, 1985), it is also very suitable for studies of the temperature dependence of the dynamics. In addition, TRX can be maintained readily in either the oxidized or reduced form for the extended periods of time often required to perform spectroscopic (especially NMR) measurements.

In this paper we report the results of ^{13}C-NMR relaxation studies of *E. coli* TRX (WT-TRX) and ^{13}C-NMR relaxation *and* trp fluorescence anisotropy studies of two functional single-trp variants of *E. coli* TRX, viz., W28F in which trp-28 is replaced by phenylalanine, and W31F in which trp-31 is replaced by phe. To enhance the NMR signal intensity for relaxation measurements and facilitate resonance assignments, we have incorporated ^{13}C-labeled trp biosynthetically into the proteins. Two different ^{13}C-enriched tryptophans, viz., $^{13}C\delta_1$-trp and $^{13}C\epsilon_3$-trp, were utilized in the sample preparations to increase the number of available NMR experimental parameters and to allow the motions of the trp rings to be monitored in the same set of experiments from the perspective of two differently oriented C-H vectors as shown in Fig. 2.

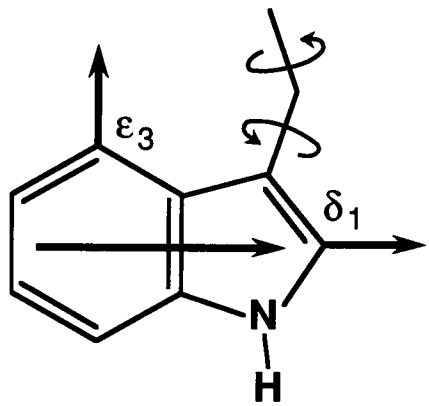

FIGURE 2 Schematic diagram of tryptophan showing the approximate directions of the $C\delta_1$-H and $C\epsilon_3$-H vectors, and the direction assumed for the fluorescence emission vector.

Three ^{13}C relaxation parameters, T_1 (the spin-lattice relaxation time), T_2 (the spin-spin relaxation time), and NOE (the steady-state nuclear Overhauser effect) were measured. For $^{13}C\delta_1$-trp and $^{13}C\epsilon_3$-trp, these quantities are dominated by the magnetic dipolar interaction of the ^{13}C nucleus with its attached proton and by the chemical shift anisotropy (CSA) of the ^{13}C. Because these interactions are modulated by the rotational motion of the molecule, information concerning that rotational motion can be obtained from relaxation data with the choice of a suitable analytic methodology such as the model-free approach of Lipari and Szabo (1982). In that approach, three motional parameters are considered, τ_m, a correlation time describing the overall rotational motion of the protein that is assumed here to be isotropic, and S^2 and τ_e, representing a measure of the amplitude and time scale, respectively, of the subnanosecond motion of a given C-H vector with respect to a reference frame fixed on the protein. S^2, the generalized order parameter, and τ_e, the effective correlation time, for the internal motion of the C-H vector are

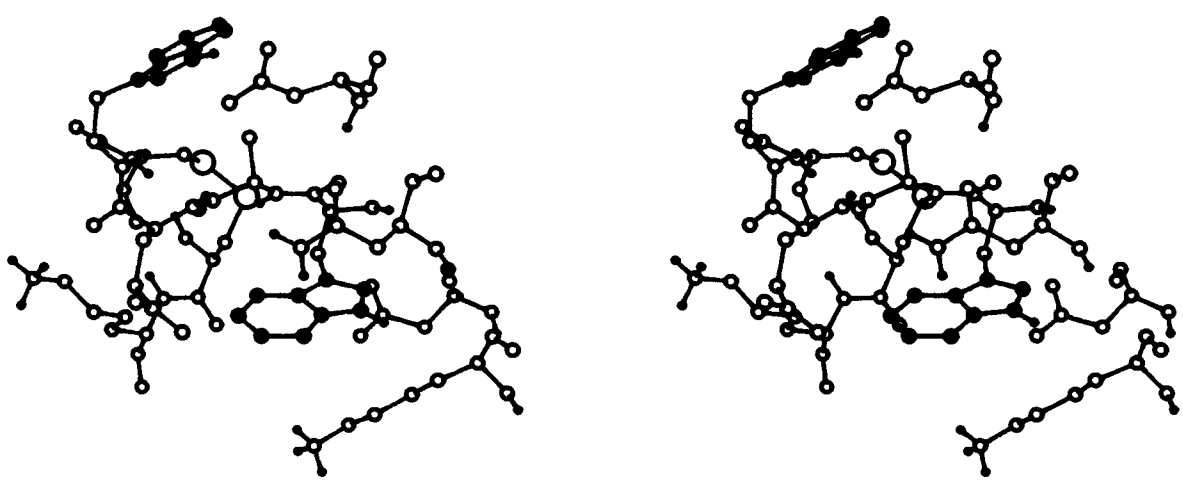

FIGURE 1 Stereo view of the residues near trp-28 and trp-31 of oxidized thioredoxin from the x-ray coordinates (Holmgren et al., 1975; Katti et al., 1990). The carbon atoms of the trp rings are represented by solid circles. Trp-31 (*upper left*) lies on the surface of the protein, and trp-28 is partially buried by a wall composed of asp-26, ala-29, glu-30, lys-36, lys-57, and asn-59. Sulfur atoms of the cys-32/cys-35 disulfide are shown enhanced in size.

independent of specific models for the motion. A primary objective of the work reported here is to examine the reliability and significance of values of S^2 and τ_e derived from relaxation data.

Tryptophan fluorescence anisotropy is also sensitive to rotational motion of the molecule. The anisotropy can be expressed in terms of parameters with similar meanings to those used to describe the ^{13}C relaxation in the NMR experiments making direct comparison of the motional information available from the NMR and fluorescence measurements feasible (Weaver et al., 1988, 1989, 1992). In the experiments described below, we have measured the steady-state and time-resolved trp fluorescence anisotropy of the mutant proteins. Because there are two trp residues in WT-TRX, there is ambiguity regarding the source of the fluorescence emission which, without accurate information on the spectral distribution and quantum yield for each trp moiety, makes it impossible to recover the contributions of each fluorophore to the measured anisotropy. This problem is obviated in the single-trp mutants. Data analysis procedures were adopted in which the steady-state anisotropy values were combined with the NMR relaxation data for $^{13}C\delta_1$-trp (Weaver et al., 1989, 1992), whereas the anisotropy decay data were analyzed separately.

The results of this work (see Kemple et al. (1993) for a preliminary account) show that, in general, the trp side chains in WT-TRX and in W31F were nearly immobile regardless of oxidation state. This is reflected in the recovery of order parameter values near 1 in those cases. A slight increase in the amplitude of the internal motion of trp-31 was observed, however, in reduced as compared with oxidized WT-TRX. At temperatures up to 50°C for WT-TRX, values for the overall correlation time decreased as expected, but there was little change in the order parameter values, indicating persistent immobilization of the trp residues. Significantly, our data did not show the general increased side-chain motion of trp-31 relative to trp-28 reported by Stone et al. (1993) from ^{15}N relaxation measurements on TRX. However, the trp-31 side chain in W28F gave indications of more freedom of motion than either trp side chain in WT-TRX or the trp-28 side chain in W31F with no noticeable dependence upon oxidation state for these mutant proteins. The increased motional freedom of trp-31 in W28F relative to trp-28 in W28F was maintained at 50°C. The agreement between the fluorescence and NMR data on W28F and W31F was generally very good with the most notable difference being that somewhat smaller values of τ_m were obtained from the time-resolved anisotropy decay data.

MATERIALS AND METHODS

Thioredoxin preparation

Thioredoxin was isolated from *Escherichia coli* strain W3110 *trp*A33 (Drapeau et al., 1968) transformed with pMS421 and a variant of pTK100. Plasmid pMS421 encodes *lacI*^{q} and spectinomycin resistance; the pTK100 derivative confers kanamycin resistance and contains a structural gene for thioredoxin under control of the *tac* promoter (Langsetmo et al., 1989). The mutant thioredoxins, W28F and W31F, were constructed by site-directed mutagenesis (Kunkel, 1985). The *Eco*RI-*Hind*III insert of pTK100 was transferred to pUC118 and was used to transform RZ1032 (F′ *lysA*$^+$/*lysA*, *dut*, *ung*, *thi*, *rel*A, *sup*E). Single-stranded DNA primers, 23 bp long, were used for site-directed mutagenesis (Kunkel, 1985). Mutants were identified by sequencing. The *Eco*RI-*Hind*III fragment was transferred into pTK100 (Langsetmo et al., 1989) and transformed into W3110 *trp*A33/pMS421 for production of mutant thioredoxin protein.

Cells were grown initially in a rich medium to which kanamycin and spectinomycin were added to select for the plasmid-bearing cells. Trp-free (acid hydrolyzed) casein and yeast extract, which contains trace quantities of trp, were included in this rich medium. The final 10-fold dilution of the cell broth was made into a medium without yeast extract. In this protocol, natural tryptophan exhaustion occurred at a cell density suitable for plasmid induction. Inducer IPTG was then added to the culture along with $^{13}C\delta_1$-trp, $^{13}C\epsilon_3$-trp (Cambridge Isotope Laboratories, Woburn, MA), or an equimolar mixture of the two. After 6 h, the cells were concentrated by centrifugation, blended in a threefold excess of pH 7.5, 20 mM TRIS, 1 mM EDTA, and sonicated. The cell debris was centrifuged and the supernatant was collected and stirred with streptomycin sulfate (1%). After a final centrifugation step, the supernatant was filtered and loaded onto a 7 liter Sephadex S-100 column. Thioredoxin fractions were identified with a colorimetric DTNB assay (Holmgren and Sjöberg, 1972), pooled, and loaded onto a 2 liter DEAE ion exchange column. Thioredoxin eluted at a KCl concentration of about 0.3 M. Protein purity was verified using silver-stained SDS PAGE PhastGel media according to manufacturer's instructions (Pharmacia LKB Biotechnology, Piscataway, NJ). The pooled fractions of oxidized protein were concentrated by ultrafiltration, dialyzed against 5 mM potassium phosphate buffer, and lyophilized. For the NMR experiments, the protein was dissolved in 99.98% D_2O to effect a sample concentration of approximately 4 mM in 50 mM, pH 6.5 or 8.0 potassium phosphate buffer. The protein samples for NMR were later reduced by adding a 5- to 10-fold molar excess of DTT. Fluorescence measurements were made on 50 mM potassium phosphate solutions with protein concentrations of 100–250 μM; a 20-fold molar excess of DTT was used to reduce the proteins for the steady-state fluorescence study, whereas for the time-resolved fluorescence anisotropy measurements a 10-fold molar excess of TCEP (Burns et al., 1991) was used. There were no indications of interconversion of the proteins between the oxidized and reduced forms during the NMR or fluorescence experiments. Also, it is worth noting that the mutant and wild-type proteins exhibited similar activity in the DTNB assay and that the mutant proteins were effectively functionally identical with WT-TRX.

NMR and fluorescence measurements

NMR measurements were conducted at the IUPUI Nuclear Magnetic Resonance Center. ^{13}C NMR signals were detected directly at 75.4 MHz on a Nicolet NT-300 FT spectrometer and on a Varian Unity 300 FT spectrometer, and at 125.7 MHz on a Varian Unity 500 FT spectrometer (Varian Associates, Palo Alto, CA). ^1H NMR measurements were performed at 300 and 500 MHz on the same spectrometers. The broadband probe used with the Unity spectrometer was obtained from Cryomagnet Systems, Inc. (Indianapolis, IN). Internal TSP (0 ppm) was used as a reference for proton spectra, and internal dioxane (67.37 ppm) was used for ^{13}C spectra. Proton-decoupled ^{13}C NMR spectra were obtained using either broadband noise or Waltz-16 (Shaka et al., 1983) decoupling during signal acquisition. Proton-coupled ^{13}C NMR spectra were acquired as well to measure differential broadening of the ^{13}C doublets (Nageswara Rao and Ray, 1992). T_1 measurements of ^{13}C were made with the inversion recovery method with proton decoupling during acquisition and normally with saturation of the proton magnetization before inversion and during recovery of the ^{13}C magnetization to eliminate cross relaxation and cross correlation effects (Boyd et al., 1990). The extracted T_1 values, which were derived from three parameter fits of the recoveries to $A\{1 - (1 + W) \cdot \exp(-t/T_1)\}$, where t is the recovery time, were the same within experimental uncertainties whether or not the proton magnetization was saturated during recovery. Steady-state ^{13}C-^1H NOE measurements were made by collecting alternate scans of the ^{13}C signals with and without nuclear Overhauser enhancement into different

memory blocks. The NOE values were obtained from ratios of the intensities or of the areas of the enhanced and equilibrium signals. T_2 measurements were made with a CPMG (Meiboom and Gill, 1958) spin echo pulse sequence with proton decoupling during acquisition only and π pulses applied to the protons at the even-numbered ^{13}C echoes (Palmer et al., 1992). The time between successive echoes was fixed at a value small compared with $1/J$ (Kay et al., 1992) to minimize the loss of magnetization due to conversion to (and subsequent decay of) anti-phase coherence (Peng et al., 1992). Three parameter, single exponential fits of the decay of the echo amplitudes were then used to extract the T_2 values. Homonuclear and heteronuclear COSY experiments were performed using now standard techniques (Piatini et al., 1982; Rance et al. 1983; Summers et al., 1986). The experimental uncertainties in T_1 and NOE are estimated to be $\pm 5\%$ and those in T_2 to be $\pm 25\%$. Chemical shifts were measured to an accuracy of ± 0.02 ppm. During the experiments, the NMR probe temperature was maintained in the range 20–50°C with a precision of ± 1°C.

Steady-state trp fluorescence anisotropy measurements were made with an SLM-4800 fluorometer (SLM Instruments, Urbana, IL) set to an excitation wavelength of 300 nm with a 1-nm bandpass. Fluorescence emission was detected through a Schott WG-345 cut-on filter (Schott Corporation, Duryea, PA). Fluorescence lifetime and time-resolved anisotropy measurements were made with a laser-based time-correlated single photon counting instrument. The instrument consists of a Coherent model 700 rhodamine dye laser pumped by a Coherent Antares mode-locked Nd-YAG laser. The dye laser output is cavity-dumped at 7.62 MHz and frequency doubled. For the lifetime measurements, the samples were excited at 295 nm and the fluorescence was detected at 360 nm through an American Holographics (Littleton, MA) monochromator. For the anisotropy decay, the samples were excited at 300 nm and the fluorescence was detected through a Spectro-Film (Winchester, MA) 350 nm optical filter with a 10-nm bandpass. The instrument response function had a full width at half maximum of 50 ps. For the anisotropy decay, a total of 3600 channels were collected at 5.3 ps per channel. The fluorescence intensity decays were resolved into discrete lifetime components by various analytical techniques (K. E. Nollet, Z. Bajzer, M. D. Kemple, and F. G. Prendergast, unpublished data) from which fraction-weighted average lifetimes were computed for use in subsequent data analysis involving the steady-state anisotropy. Anisotropy decays were analyzed using a global approach that included the instrument response function and the fluorescence intensity decay (Beechem and Gratton, 1988). The sample temperature for these measurements was 20°C.

Data analysis-NMR

Because the primary ^{13}C relaxation mechanisms in this case consist of the ^{13}C-^1H magnetic dipolar interaction (DD) and the ^{13}C chemical shift anisotropy (CSA), T_1, T_2, and the NOE are given in terms of the following equations (Abragam, 1961; Lipari and Szabo, 1982).

$$T_1^{-1} = R_{DD}^{(1)} + R_{CSA}^{(1)}, \tag{1}$$

$$T_2^{-1} = R_{DD}^{(2)} + R_{CSA}^{(2)}, \tag{2}$$

and

$$\mathrm{NOE} = 1 + \frac{1}{4}\alpha^2\left(\frac{\gamma_H}{\gamma_C}\right)\left[\frac{6J(\omega_H + \omega_C) - J(\omega_H - \omega_C)}{R_{DD}^{(1)} + R_{CSA}^{(1)}}\right], \tag{3}$$

where

$$R_{DD}^{(1)} = \tfrac{1}{4}\alpha^2[J(\omega_H - \omega_C) + 3J(\omega_C) + 6J(\omega_H + \omega_C)], \tag{4}$$

$$R_{CSA}^{(1)} = \tfrac{1}{3}\beta^2 J(\omega_C), \tag{5}$$

$$R_{DD}^{(2)} = \tfrac{1}{8}\alpha^2[4J(0) + J(\omega_H - \omega_C) + 3J(\omega_C) + 3J(\omega_H) + 6J(\omega_H + \omega_C)], \tag{6}$$

$$R_{CSA}^{(2)} = \tfrac{1}{18}\beta^2[4J(0) + 3J(\omega_C)], \tag{7}$$

with

$$\alpha = \frac{\gamma_C\gamma_H\hbar}{r_{CH}^3} \quad \text{and} \quad \beta = \frac{3}{2}\omega_C\,\delta_{ZZ}\left(1 + \frac{\zeta^2}{3}\right)^{1/2}.$$

ω_C and ω_H are the carbon and proton resonance frequencies, γ_C and γ_H are their respective gyromagnetic ratios; $\hbar$ is Planck's constant over 2π, r_{CH} is the carbon-proton distance, δ_{ZZ} is the largest magnitude principal element of the carbon CSA tensor (in ppm), and ζ is the asymmetry parameter of the CSA tensor. Numerical values of the CSA tensor quantities for $^{13}C\delta_1$-trp and $^{13}C\epsilon_3$-trp are given below.

The spectral density, $J(\omega)$, originally suggested by Lipari and Szabo (1982), is used to relate the relaxation to the molecular motion according to

$$J(\omega) = \frac{2}{5}\left\{\frac{S^2\tau_m}{1 + \omega^2\tau_m^2} + \frac{(1 - S^2)\tau}{1 + \omega^2\tau^2}\right\} \tag{8}$$

where S^2 is a generalized, motional model-free order parameter dependent on the amplitude of the internal motion of the C-H vector ($0 \le S^2 \le 1$), and $\tau^{-1} = \tau_m^{-1} + \tau_e^{-1}$ consists of τ_e, an effective correlation time for the internal motion, which has meaning when $S^2 < 1$, and of τ_m, a correlation time for the overall rotational motion of the molecule. Only a single parameter (τ_m) is used to characterize the overall motion because that motion is expected to be essentially isotropic for TRX, which has a shape that does not deviate appreciably from spherical. Values of τ_m, S^2, and τ_e can be found from the measured relaxation rates by substituting Eq. 8 for the spectral density into Eqs. 1–7 and treating τ_m, S^2, and τ_e as fitting parameters. There are many examples of investigations of rotational dynamics by ^{13}C and ^{15}N relaxation measurements employing a number of analysis techniques. (See, for example, Barbato et al., 1992; Clore et al., 1990b; Dellwo and Wand, 1989; Matthews et al., 1993; Palmer et al., 1991; Peng and Wagner, 1992; Schneider et al., 1992; Stone et al. 1993; Weaver et al., 1989.) Details of the specific procedures followed in our analysis are given in the Results section.

When the CSA as well as the ^{13}C-^1H dipolar interactions make significant contributions to the relaxation rates, the interference of those interactions, called cross correlation, may be manifested as a differential broadening of the components of the ^{13}C multiplet in ^1H-coupled spectra (Goldman, 1984; Nageswara Rao and Ray, 1992). For a single attached proton as is the case for $^{13}C\delta_1$-trp and $^{13}C\epsilon_3$-trp, the difference in width between the two lines of a given ^{13}C doublet, $\Delta(LW)$ in Hz, can be written as (Nageswara Rao and Ray, 1992)

$$\Delta(LW) = \frac{1}{6\pi}\alpha\beta'[4J(0) + 3J(\omega_C)] \tag{9}$$

with

$$\beta' = \tfrac{3}{2}\omega_C\,\delta_{ZZ}[3\cos^2\theta - 1 - \zeta\sin^2\theta\cos 2\phi].$$

θ and ϕ are spherical coordinates of the C-H bond in the principal axis frame of the CSA tensor. The other symbols were defined above. The spectral density in Eq. 9 is a cross-correlation spectral density and is not formally identical to that given by Eq. 8 unless $\theta = 0$ (Elbayed and Canet, 1989). However, θ is near zero for both ^{13}C labels considered (see below). Therefore, the spectral density of Eq. 8 can be used with Eq. 9 with the expectation that serious error will not be incurred, allowing differential broadening to become another measure of the motional parameters.

A major goal of this work is to ascertain if picosecond internal motions in proteins can be measured reliably. Simulations of ^{13}C relaxation data indicate that the NOE is generally more sensitive to τ_e than either T_1 or T_2 especially for order parameter values approaching 1, which was often the case here and which has been found generally in proteins. Explicit examples of the τ_e dependence of T_1 and NOE are shown in Fig. 3 for $^{13}C\delta_1$-trp calculated with a $\tau_m = 10$ ns and $S^2 = 0.81$. Although T_1 is only weakly dependent on τ_e at 75.4 MHz, it is more sensitive at 125.7 MHz because the corresponding larger value of $\omega\tau_m$ reduces the importance of the first term in $J(\omega)$ relative to the second (Eq. 8). Fig. 3 clearly confirms that at both

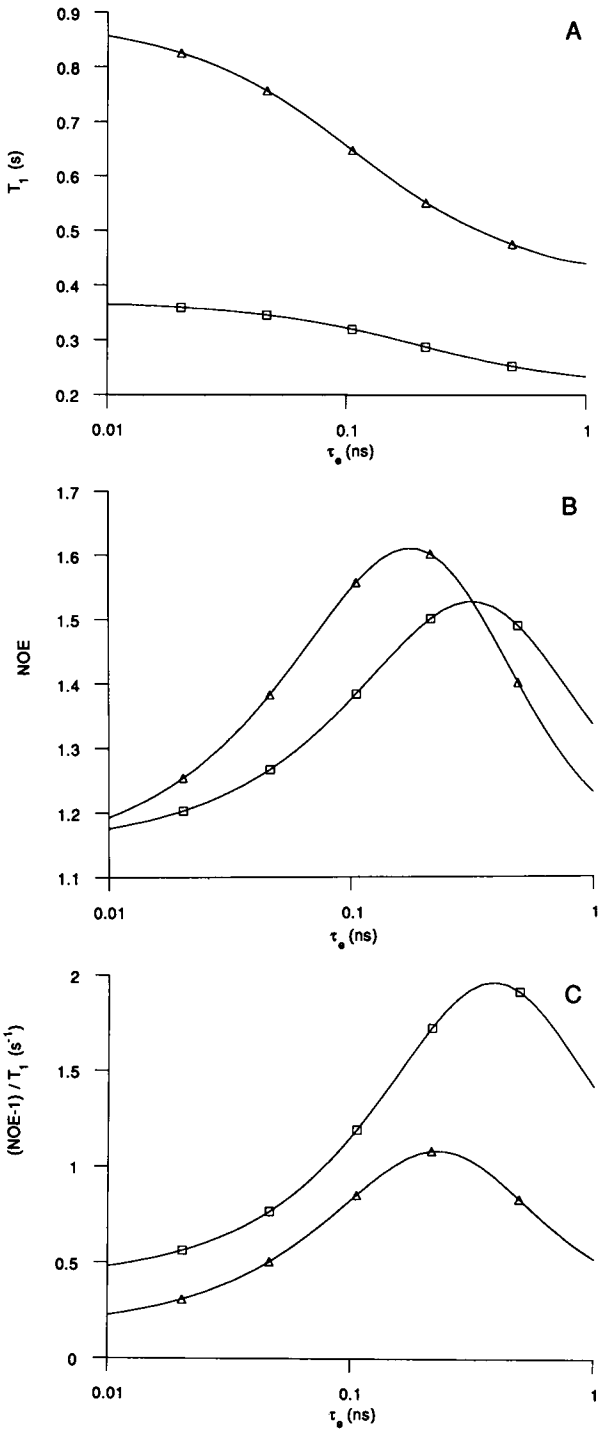

FIGURE 3 ^{13}C T_1 (panel *A*), steady state NOE (panel *B*), and (NOE-1)/T_1 (panel *C*) data simulated as a function of τ_e for $^{13}C\delta_1$-trp with τ_m = 10 ns and S^2= 0.81 at 75.4 MHz (△) and 125.7 MHz (□). Equations 1–8 and 10 in the text were used in the simulations. The symbols shown on the curves simply serve as labels.

frequencies the NOE is more sensitive to τ_e than is T_1. On the other hand, T_2 (not shown) is nearly independent of τ_e.

It can be seen that the τ_e sensitivity of the NOE originates in the cross-relaxation term, traditionally called σ when the NOE is written as $1 + (\gamma_H/\gamma_C)(\sigma/\rho)$ with $\rho = T_1^{-1}$. However, the presence of T_1 in the NOE expression somewhat mutes the dependence of the NOE on τ_e. On the other hand, the quantity (NOE − 1)/T_1, which can be written

$$(\text{NOE} - 1)/T_1 = \frac{1}{4}\alpha^2\left(\frac{\gamma_H}{\gamma_C}\right)[6J(\omega_H + \omega_C) - J(\omega_H - \omega_C)], \quad (10)$$

is directly proportional to σ and could be expected to be yet more sensitive to τ_e. This expectation is borne out in the plot of (NOE − 1)/T_1 vs. τ_e shown in Fig. 3 *C*. Fractional changes in (NOE − 1)/T_1 are much greater than those in the NOE for the same variation in τ_e. Moreover, if there are any unaccounted for additional relaxation processes contributing to T_1, they may reduce the measured NOE values and increase the difficulty in extracting consistent values for the motional parameters especially when the measured NOE approaches the rigid-molecule limiting value, which is the case for the results reported here (see below). For these reasons, the motional parameters reported below for TRX were obtained with (NOE − 1)/T_1 replacing NOE in the analysis. Dellwo and Wand (1989) followed a similar procedure, not necessarily for the same reasons, in their analysis of NMR relaxation data by including NOE/T_1 in the target function used in their fitting procedure.

Data analysis-fluorescence

In analogy to the correlation function used for the C-H vector in the NMR analysis (Lipari and Szabo, 1982), the time-dependent fluorescence anisotropy, $r(t)$, can be written

$$r(t)/r_o = \exp(-t/\tau_m)\,(S^2 + (1 - S^2)\exp(-t/\tau_e)), \quad (11)$$

where the correlation times have the same meaning as above, and $S^2 = r_\infty/r_o$ is an orientational order parameter. r_o is the fundamental anisotropy, which is a function of the relative orientation of the fluorescence emission and absorption dipoles at a given excitation wavelength and r_∞ is the limiting hindered anisotropy of the fluorophore. The time-resolved anisotropy data were fitted directly to Eq. 11 with r_0, S^2, τ_m, and τ_e treated as adjustable parameters. Alternatively, an expression for the steady-state anisotropy, $\bar{r}$, can be obtained from Eq. 11 with the assumption of a single fluorescence lifetime, τ_f, viz., (Weaver et al., 1989)

$$\bar{r}/r_o = \frac{(1 - S^2)}{1 + \tau_f(\tau_e^{-1} + \tau_m^{-1})} + \frac{S^2}{1 + (\tau_f/\tau_m)}. \quad (12)$$

The fluorescence-derived order parameter S^2 and the NMR-derived order parameter S^2 are expected to be the same only when the emission dipole is colinear with the relevant C-H vector. Although the indole ring deviates somewhat from planarity, and the direction of the trp emission vector is not well known (e.g., see Lakowicz et al. (1983) and Ruggiero et al. (1990) for references and depictions of the trp fluorescence emission dipole vector), colinearity of the C-H and fluorescence emission vectors appears to be more nearly met for $C\delta_1$-H than for $C\epsilon_3$-H. Hence, for the purposes of our data analysis, the $C\delta_1$-H vector will be considered to be parallel to the fluorescence emission dipole vector as indicated in Fig. 2 and $\bar{r}$ will be combined with the NMR relaxation data for $C\delta_1$ only, where appropriate. Also, although fluorescence intensity decays seldom can be described by a single exponential function, calculations (unpublished) show that inclusion of a multi-exponential form for the fluorescence intensity decay in the derivation of Eq. 12 generally does not have a consequential effect on the motional parameters obtained from the steady-state anisotropy and that it is sufficient to use the average fluorescence lifetime $\langle\tau_f\rangle$ for τ_f in Eq. 12.

Numerical values used in the analysis with the equations above (other than standard values for the fundamental constants) were: r_{CH} = 1.09 Å; CSA tensor elements for $^{13}C\delta_1$-trp and $^{13}C\epsilon_3$-trp, respectively (Separovic et al., 1991 and unpublished results), δ_{ZZ} = −78 ppm, ζ = 0.936, θ = 26°, ϕ = 90°; δ_{ZZ} = −115 ppm, ζ = 0.639, θ = 0°; r_0 is discussed below. The (weak) temperature dependence of the CSA tensor was not taken into account in the analysis; this dependence should have only a very small effect on the relaxation rates.

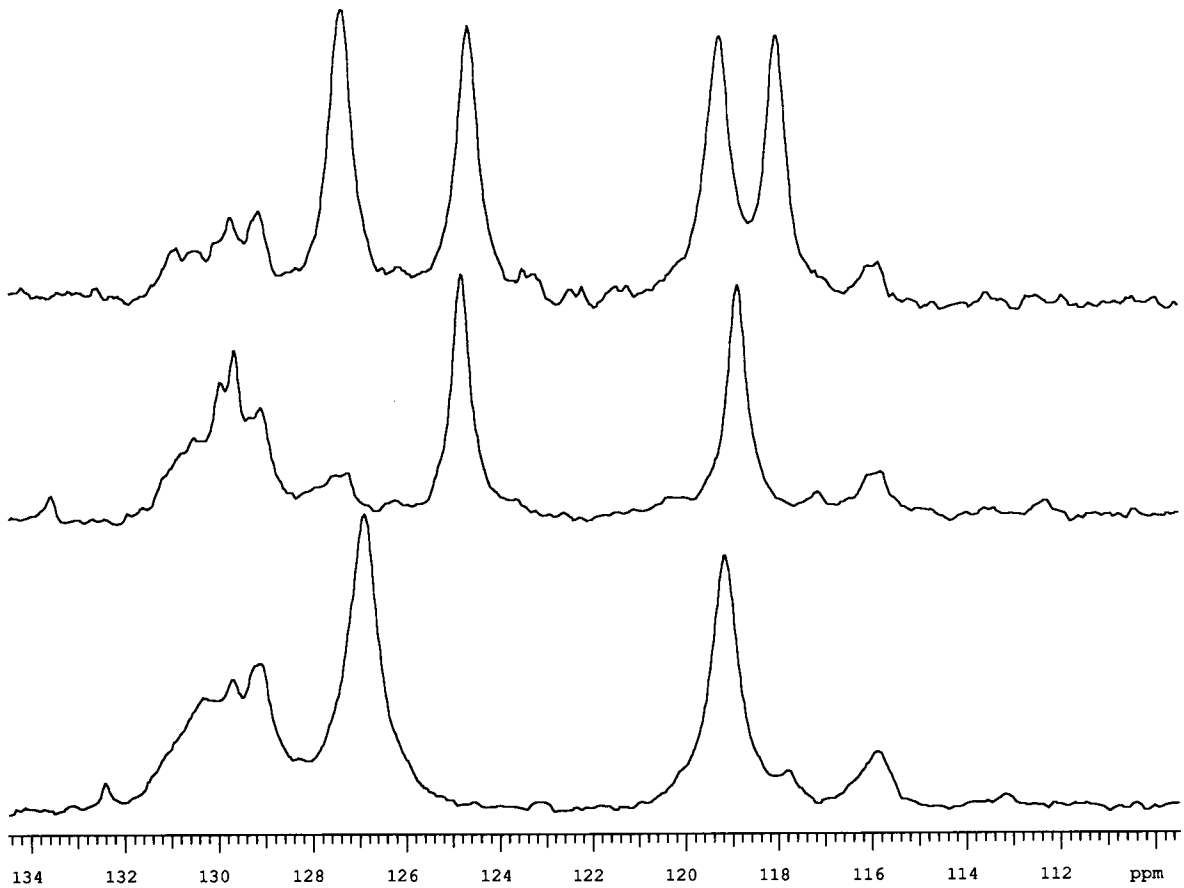

FIGURE 4 Proton-decoupled ^{13}C NMR spectra of oxidized WT-TRX (*top*), W31F (*middle*), and W28F (*bottom*) obtained at 75.4 MHz. The spectra are referenced to internal dioxane at 67.37 ppm. Signals from $^{13}C\delta_1$-trp are in the range 124.4–127 ppm, whereas signals from $^{13}C\epsilon_3$-trp are in the range 118–119.2 ppm. The sample conditions were concentration ~5 mM, pH 6.5, and temperature 20°C.

RESULTS

Single-pulse and COSY ^1H-NMR spectra (not shown) of WT-TRX, W28F, and W31F were obtained at 300 and 500 MHz. Overall, the spectra were quite similar among the three proteins, and the WT-TRX spectra were consistent with published *E. coli* TRX assignments (LeMaster and Richards, 1988; Dyson, et al., 1989). The efficiency of incorporation of the ^{13}C-labeled tryptophans was estimated to be about 90% by comparison of ^1H signals from unlabeled trp with isolated signals from other residues. The presence of labeled trp was apparent in ^{13}C NMR spectra as shown in Fig. 4, which is a superposition of proton-decoupled ^{13}C spectra of oxidized WT-TRX, W28F, and W31F. Because these samples have two isotopically labeled tryptophans, namely $^{13}C\delta_1$-trp and $^{13}C\epsilon_3$-trp, a proton-decoupled ^{13}C spectrum of WT-TRX consists of four lines. In all cases, the decoupled ^{13}C signals from trp-28 and trp-31 were resolved. ^{13}C resonance assignments in the proteins were made by comparison with spectra of free $^{13}C\delta_1$-trp and $^{13}C\epsilon_3$-trp and by use of published ^1H chemical shift assignments for trp in *E. coli* TRX (Dyson et al., 1989). Specifically, the chemical shifts of the protons directly attached to the ^{13}C nuclei were measured and then identified from heteronuclear COSY spectra, an example of which is shown in Fig. 5 for oxidized WT-TRX. The assigned ^{13}C chemical shifts in the WT protein were consistent with the chemical shifts observed in spectra of the single-trp mutants (Fig. 4 and Tables 1–3). In general, for a given labeled position in the indole ring, the ^{13}C signals from trp-31 were downfield of the trp-28 signals.

^{13}C relaxation rates were measured for oxidized and reduced WT-TRX at pH 6.5 at both 75.4 and 125.7 MHz and at 20, 25, 35, and 50°C. Relaxation data for oxidized and reduced WT-TRX and W28F at pH 8.0 were taken only at 75.4 MHz and 20°C. Data for oxidized W28F and W31F at pH 6.5 were taken at 75.4 MHz and 20°C, and at both 20 and 50°C for the reduced proteins. For WT-TRX the relaxation data and chemical shift information are given in Tables 1 and 2. Fluorescence steady-state anisotropy and lifetime data obtained at 20°C are included with the NMR data for the mutant proteins in Table 3. Note that T_2 was measured in a limited number of cases only.

There are a number of factors in the data analysis that warrant consideration. The first concerns the parameter τ_m, the correlation time for the overall rotational motion of the protein. Among T_1, T_2, and NOE for proteins, T_2 is the most crucial for determining τ_m because of the $J(0)$ term in Eqs.

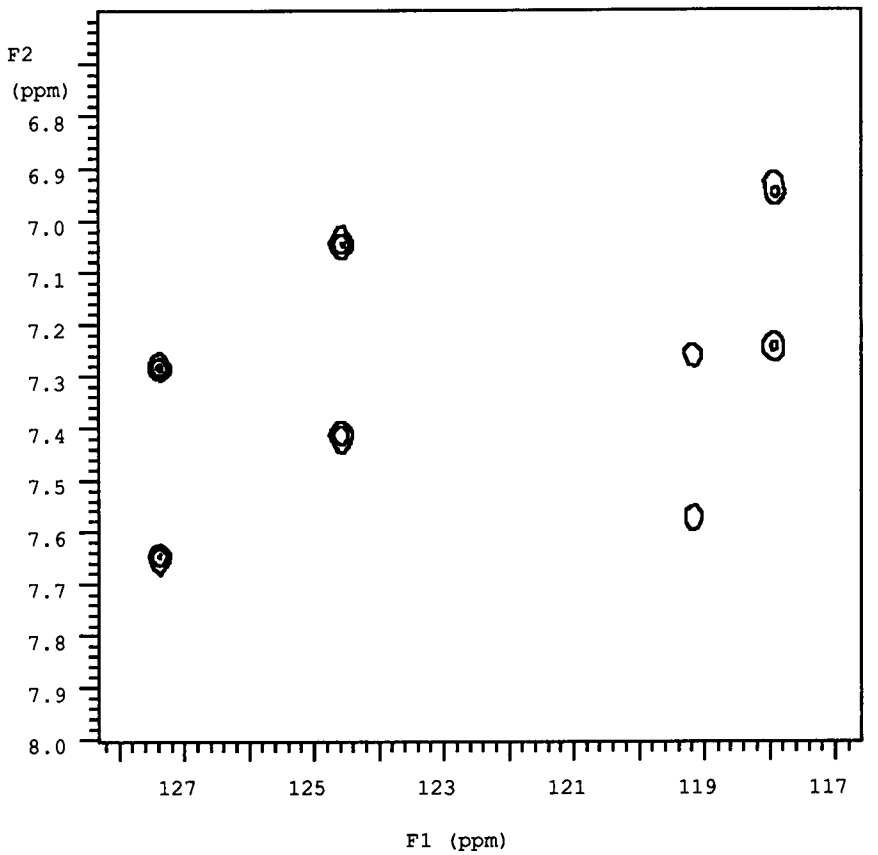

FIGURE 5 ^{13}C-^{1}H correlation spectrum of oxidized WT-TRX obtained at 499.8 MHz. In F1 (^{13}C), 128 points were sampled in a spectral width of 2514 Hz, whereas in F2 (^{1}H), 4K points were sampled in the hypercomplex mode in a spectral width of 6000 Hz. The resulting data matrix was zero-filled to 256 × 4K. The spectrum is proton decoupled in F1 and ^{13}C-coupled in F2. ^{13}C chemical shifts are referenced to internal dioxane at 67.37 ppm; proton chemical shifts are referenced to TSP at 0 ppm. The sample conditions were concentration ~5 mM, pH 6.5, and temperature 25°C.

6 and 7. However, problems with the interpretation of measured T_2 values have been encountered. Various authors (see, for example, Cheng et al., 1993; Clore et al., 1990b; Palmer et al., 1991; Redfield et al., 1992; Stone et al., 1993) have found it necessary to add correlation-time-independent terms to the expression for T_2^{-1} to account for chemical/conformational exchange at some molecular sites, especially in ^{15}N experiments. Because the added term will take on whatever value necessary to cause T_2^{-1} to be fit exactly, this procedure effectively eliminates those T_2 data from the τ_m determination. Furthermore, T_2 experiments must be designed carefully to minimize effects from cross correlation of the CSA and dipolar interactions and from contributions due to the relaxation of anti-phase coherence. In our analyses, wherever T_2 values were available, they either were included with no additional terms in Eq. 2 or they were omitted altogether. It was *always* the case that larger values of τ_m were found when T_2 was included (see Tables 4 and 5).

A second factor is that the NOE values obtained (Tables 1–3) are close to their rigid-molecule limiting values (i.e., those applicable when there is no internal motion), as mentioned above, even for sample temperatures of 50°C. In particular with $S = 1$ and $\tau_m = 10$ ns, the calculated limiting NOE values for $^{13}C\delta_1$-trp and $^{13}C\epsilon_3$-trp are 1.15 and 1.14 at 75.4 MHz, respectively, and 1.13 and 1.11 at 125.7 MHz. Similarly, the corresponding values with $\tau_m = 5$ ns are 1.17 and 1.16 at 75.4 MHz and 1.14 and 1.12 at 125.7 MHz. The proximity of the measured NOE values to the limiting values, especially in WT-TRX, made it difficult to fit the relaxation equations to the data without placing some (physically reasonable) restrictions on the range of parameter values. Generally the relaxation data were better fit when NOE was replaced with (NOE − 1)/T_1 in the analysis, and only those results are given in the following tables. Trends in the motional parameters were similar whether (NOE − 1)/T_1 or NOE was used. For example, Table 1 shows that for reduced WT-TRX at pH 6.5, trp-31 consistently had slightly larger NOE values than trp-28 giving evidence for the presence of some, albeit limited, internal motion. Larger NOE values were generally reflected in smaller order parameter values in the analysis. Interestingly for W28F (Table 3), the NOE data clearly indicate more motional freedom for the trp-31 in this protein than is the case for either trp-31 or trp-28 in WT-TRX.

Third, because WT-TRX has two tryptophan residues, it is impossible to associate unambiguously the fluorescence anisotropy with a specific residue. Therefore, $\bar{r}$ was combined with the NMR data in the analysis only for $^{13}C\delta_1$-trp in the mutant proteins (at 20°C). Attempts to use quantum-yield weighted values of $\bar{r}$ for analysis of WT-TRX data were not fruitful.

Motional parameters extracted from the relaxation data by nonlinear least-squares fitting procedures of the relaxation data to Eqs. 1–8 and 10 using the computer program, nyep (P. Buckley, private communication), are summarized in Tables 4–6 for WT-TRX. Results for W28F and W31F, ana-

TABLE 1 Relaxation data for WT-TRX at pH 6.5

			75.4 MHz			125.7 MHz	
T	Nucleus	δ	T_1	T_2	NOE	T_1	NOE
°C		ppm	s	s		s	
			Oxidized Protein				
20	$C\delta_1$-W28	124.61	0.313	0.015	1.15	0.600	1.18
	$C\epsilon_3$-W28	117.97	0.328	0.017	1.14	0.543	1.16
	$C\delta_1$-W31	127.37	0.317	0.017	1.16	0.611	1.15
	$C\epsilon_3$-W31	119.22	0.297	0.014	1.16	0.548	1.15
25	$C\delta_1$-W28	124.63	0.245	—	1.17	0.547	1.16
	$C\epsilon_3$-W28	118.02	0.270	—	1.16	0.478	1.14
	$C\delta_1$-W31	127.38	0.261	—	1.14	0.572	1.12
	$C\epsilon_3$-W31	119.22	0.248	—	1.15	0.495	1.12
35	$C\delta_1$-W28	124.63	0.196	—	1.15	0.436	1.10
	$C\epsilon_3$-W28	118.04	0.195	—	1.17	0.370	1.11
	$C\delta_1$-W31	127.42	0.228	—	1.15	0.443	1.09
	$C\epsilon_3$-W31	119.21	0.221	—	1.15	0.381	1.10
50	$C\delta_1$-W28	124.64	0.190	0.029	1.17	0.320	1.12
	$C\epsilon_3$-W28	118.09	0.163	0.017	1.18	0.278	1.11
	$C\delta_1$-W31	127.44	0.176	0.024	1.14	0.359	1.10
	$C\epsilon_3$-W31	119.21	0.148	0.018	1.15	0.310	1.10
			Reduced Protein				
20	$C\delta_1$-W28	124.73	0.261	0.017	1.19	0.642	1.10
	$C\epsilon_3$-W28	118.04	0.297	0.013	1.11	0.563	1.09
	$C\delta_1$-W31	127.23	0.295	0.018	1.27	0.682	1.22
	$C\epsilon_3$-W31	119.48	0.266	0.016	1.21	0.585	1.18
25	$C\delta_1$-W28	124.74	0.273	—	1.18	0.560	1.11
	$C\epsilon_3$-W28	118.07	0.270	—	1.16	0.512	1.10
	$C\delta_1$-W31	127.27	0.295	—	1.22	0.581	1.19
	$C\epsilon_3$-W31	119.50	0.279	—	1.19	0.494	1.15
35	$C\delta_1$-W28	124.74	0.211	—	1.18	0.483	1.13
	$C\epsilon_3$-W28	118.10	0.203	—	1.14	0.369	1.10
	$C\delta_1$-W31	127.28	0.237	—	1.19	0.475	1.15
	$C\epsilon_3$-W31	119.50	0.235	—	1.14	0.385	1.16
50	$C\delta_1$-W28	124.72	0.191	0.026	1.19	0.354	1.15
	$C\epsilon_3$-W28	118.12	0.174	0.028	1.20	0.297	1.09
	$C\delta_1$-W31	127.30	0.192	0.026	1.18	0.354	1.16
	$C\epsilon_3$-W31	119.47	0.184	0.020	1.17	0.308	1.15

TABLE 2 Relaxation data for WT-TRX at pH 8.0, 20°C, and 75.4 MHz

Nucleus	δ	T_1	NOE
	ppm	s	
	Oxidized Protein		
$C\delta_1$-W28	124.61	0.35	1.22
$C\epsilon_3$-W28	118.18	0.34	1.12
$C\delta_1$-W31	127.47	0.36	1.19
$C\epsilon_3$-W31	119.29	0.33	1.38
	Reduced Protein		
$C\delta_1$-W28	124.60	0.29	1.15
$C\epsilon_3$-W28	118.36	0.30	1.11
$C\delta_1$-W31	127.20	0.27	1.16
$C\epsilon_3$-W31	119.38	0.31	1.13

lyzed with the inclusion of Eq. 12, are given in Table 7. For the WT protein, an iterative procedure was followed in which the order parameters were first fixed to find τ_m. Subsequently, τ_m was fixed and S^2 and τ_e were found. For W28F and W31F, when $\bar{r}$ and $\langle\tau_f\rangle$ were available, τ_m was determined from the $^{13}C\delta_1$-trp relaxation data including $\bar{r}$ and $\langle\tau_f\rangle$ and subsequently used to find the other parameters. If there were no fluorescence data, the procedure used for WT-TRX was followed for W28F and W31F. Typically, a range of τ_m values of $\pm$1.5 ns at 20 and 25°C, and $\pm$0.5 ns at 35 and 50°C led to fits of the relaxation data within the experimental errors. It was found that S^2 generally increased with τ_m for a given set of data, but, more importantly, the relative S^2 values among the four labels were maintained. The final order parameters obtained are estimated to be reliable to within $\pm$0.06 in the absolute sense and to within $\pm$0.04 in a relative sense. The appropriateness of the τ_e values is difficult to ascertain, especially when the order parameters approach 1. Errors generated by the computer program based on the goodness of the fit and the sensitivity of the fitting procedure to τ_e generally indicated variations on the order of $\pm$20–50%.

The motional parameters obtained for W28F and W31F were sensitive to the value chosen for r_o when the fluorescence data were included. Therefore, results obtained with two different values of r_o, viz., 0.26 and 0.31, are given in Table 7. There is not consensus in the fluorescence literature with regard to the value that is appropriate for r_o. Those chosen here encompass the range of values given by Ruggiero et al. (1990) with 0.31 also coinciding with the value determined by Valeur and Weber (1977). They are also consistent with values obtained from our time resolved anisotropy data (Table 9). As seen from Table 7, the larger value

TABLE 3 Chemical shift, relaxation data at 75.4 MHz, steady-state fluorescence anisotropy, and average fluorescence lifetime for the mutant proteins

Sample	T	pH	Nucleus	δ	T_1	T_2	NOE	$\bar{r}$*	$\langle\tau_f\rangle$
	°C			ppm	s	s			ns‡
				Oxidized Proteins					
W31F	20	6.5	$C\delta_1$-W28	124.82	0.355	—	1.15	0.209	3.04
W31F			$C\epsilon_3$-W28	118.89	0.373	—	1.18		
W28F			$C\delta_1$-W31	126.90	0.429	0.010	1.25	0.137	2.37
W28F			$C\epsilon_3$-W31	119.16	0.410	0.008	1.21		
W28F		8.0	$C\delta_1$-W31	127.21	0.400	—	1.24	0.138	2.72
W28F			$C\epsilon_3$-W31	119.21	0.370	—	1.23		
				Reduced Proteins					
W31F	20	6.5	$C\delta_1$-W28	124.71	0.385	—	1.19	0.175	5.08
W31F			$C\epsilon_3$-W28	118.57	0.365	—	1.15		
W28F			$C\delta_1$-W31	126.58	0.430	0.009	1.21	0.154	2.05
W28F			$C\epsilon_3$-W31	119.37	0.406	0.007	1.22		
W28F		8.0	$C\delta_1$-W31	126.67	0.434	0.011	1.24	0.140	2.19
W28F			$C\epsilon_3$-W31	119.35	0.432	0.009	1.24		
W31F	50	6.5	$C\delta_1$-W28	124.71	0.232	—	1.16		
W31F			$C\epsilon_3$-W28	118.49	0.187	—	1.15		
W28F			$C\delta_1$-W31	127.00	0.258	0.017	1.21		
W28F			$C\epsilon_3$-W31	119.23	0.217	0.015	1.18		

* Measured with an excitation wavelength of 300 nm.
‡ Measured with an excitation wavelength of 295 nm.

TABLE 4 Motional parameters obtained for oxidized WT-TRX at pH 6.5

	Nucleus	τ_m	τ_e	S^2
		ns	ns	
20°C T_2 included	$C\delta_1$-W28	8.71	0.053	0.96
	$C\epsilon_3$-W28	8.71	0.018	0.88
	$C\delta_1$-W31	8.71	0.030	0.97
	$C\epsilon_3$-W31	8.71	0.048	0.97
20°C without T_2	$C\delta_1$-W28	8.39	0.015	0.84
	$C\epsilon_3$-W28	8.39	0.011	0.76
	$C\delta_1$-W31	8.39	0.009	0.85
	$C\epsilon_3$-W31	8.39	0.013	0.84
25°C without T_2	$C\delta_1$-W28	7.65	0.078	0.98
	$C\epsilon_3$-W28	7.65	0.015	0.87
	$C\delta_1$-W31	7.65	0	0.91
	$C\epsilon_3$-W31	7.65	0.008	0.93
35°C without T_2	$C\delta_1$-W28	6.58	—	1.00
	$C\epsilon_3$-W28	6.58	2.69	0.94
	$C\delta_1$-W31	6.58	0.001	0.90
	$C\epsilon_3$-W31	6.58	0	0.96
50°C T_2 included	$C\delta_1$-W28	5.27	0.151	0.99
	$C\epsilon_3$-W28	5.27	1.68	0.95
	$C\delta_1$-W31	5.27	—	1.00
	$C\epsilon_3$-W31	5.27	—	1.00
50°C without T_2	$C\delta_1$-W28	4.97	0.014	0.96
	$C\epsilon_3$-W28	4.97	3.15	0.92
	$C\delta_1$-W31	4.97	0	0.89
	$C\epsilon_3$-W31	4.97	—	1.00

TABLE 5 Motional parameters obtained for reduced WT-TRX at pH 6.5

	Nucleus	τ_m	τ_e	S^2
		ns	ns	
20°C T_2 included	$C\delta_1$-W28	8.08	—	1.00
	$C\epsilon_3$-W28	8.08	0	0.82
	$C\delta_1$-W31	8.08	0.349	0.97
	$C\epsilon_3$-W31	8.08	0.244	0.98
20°C without T_2	$C\delta_1$-W28	7.79	0	0.94
	$C\epsilon_3$-W28	7.79	0	0.73
	$C\delta_1$-W31	7.79	0.031	0.85
	$C\epsilon_3$-W31	7.79	0.024	0.86
25°C without T_2	$C\delta_1$-W28	7.68	0	0.94
	$C\epsilon_3$-W28	7.68	0	0.89
	$C\delta_1$-W31	7.68	0.025	0.86
	$C\epsilon_3$-W31	7.68	0.019	0.86
35°C without T_2	$C\delta_1$-W28	6.24	0	0.98
	$C\epsilon_3$-W28	6.24	0	0.95
	$C\delta_1$-W31	6.24	0.015	0.90
	$C\epsilon_3$-W31	6.24	0.020	0.82
50°C T_2 included	$C\delta_1$-W28	4.94	0.122	0.99
	$C\epsilon_3$-W28	4.94	—	1.00
	$C\delta_1$-W31	4.94	0.094	0.98
	$C\epsilon_3$-W31	4.94	0.090	0.97
50°C without T_2	$C\delta_1$-W28	4.73	0.019	0.90
	$C\epsilon_3$-W28	4.73	0	0.96
	$C\delta_1$-W31	4.73	0.021	0.88
	$C\epsilon_3$-W31	4.73	0.025	0.86

of r_o yields a smaller value for τ_m and a correspondingly smaller S^2. In the extreme, fits using the theoretical maximum $r_o = 0.4$ (results not shown) gave unreasonably small τ_m values. Order parameter values were more consistent with those obtained from steady-state anisotropy alone and with the time-resolved anisotropy data (see below) with $r_o = 0.26$ than with $r_0 = 0.31$, especially for W31F.

The differential broadening, $\Delta(LW)$, of the ^{13}C doublets in the proteins was measured from proton-coupled spectra under various conditions, and $\Delta(LW)$ values for WT-TRX at 125.7 MHz are given in Table 8. Data for WT-TRX at 75.4 MHz were reported elsewhere (Kemple et al., 1993). Reliable differential broadening data for the mutant proteins were more difficult to obtain because of sensitivity considerations and overlap of signals from naturally abundant ^{13}C in other residues. At higher sample temperatures, $\Delta(LW)$ decreased as expected and $\Delta(LW)$ is smaller for $^{13}C\delta_1$-trp than for $^{13}C\epsilon_3$-trp under the same sample conditions due to the smaller CSA of $^{13}C\delta_1$-trp. For order parameter values approaching 1, it can be shown from Eqs. 8 and 9 that $\Delta(LW)$ is given

TABLE 6 Motional parameters obtained for WT-TRX at pH 8.0 and 20°C. T_2 was not included in the analysis*

	Nucleus	τ_m	τ_e	S^2
		ns	ns	
Oxidized protein	$C\delta_1$-W28	10.5	0.039	0.87
	$C\epsilon_3$-W28	10.5	0	0.87
	$C\delta_1$-W31	10.5	0.021	0.86
Reduced protein	$C\epsilon_3$-W28	10.1	0	0.84
	$C\delta_1$-W31	10.1	4.13	0.91
	$C\epsilon_3$-W31	10.1	0	0.89

* Physically reasonable values for the parameters consistent with the other labels could not be obtained for $C\epsilon_3$-W31 in the oxidized protein and $C\delta_1$-W28 in the reduced protein and are not shown.

TABLE 7 Motional parameters obtained for the single-trp mutants of TRX. T_2 was not included in the analysis

Sample	Nucleus	τ_m	τ_e	S^2
		ns	ns	
W31F, Oxidized	$C\delta_1$-W28	12.1	2.27	0.99
20°C, pH 6.5	$C\epsilon_3$-W28	12.1	0.025	0.89
r_0 = 0.26				
W31F, Oxidized	$C\delta_1$-W28	10.3	0.001	0.87
20°C, pH 6.5	$C\epsilon_3$-W28	10.3	0.012	0.77
r_0 = 0.31				
W31F, Reduced	$C\delta_1$-W28	12.5	0.053	0.94
20°C, pH 6.5	$C\epsilon_3$-W28	12.5	0.019	0.95
r_0 = 0.26				
W31F, Reduced	$C\delta_1$-W28	10.9	0.016	0.83
20°C, pH 6.5	$C\epsilon_3$-W28	10.9	0.005	0.84
r_0 = 0.31				
W31F, Reduced	$C\delta_1$-W28	4.86	0	0.69
50°C, pH 6.5	$C\epsilon_3$-W28	4.86	0	0.81
W28F, Oxidized	$C\delta_1$-W31	9.79	0.017	0.65
20°C, pH 6.5	$C\epsilon_3$-W31	9.79	0.012	0.65
r_0 = 0.26				
W28F, Oxidized	$C\delta_1$-W31	8.35	0.013	0.56
20°C, pH 6.5	$C\epsilon_3$-W31	8.35	0.010	0.57
r_0 = 0.31				
W28F, Oxidized	$C\delta_1$-W31	9.46	0.018	0.68
20°C, pH 8	$C\epsilon_3$-W31	9.46	0.020	0.69
r_0 = 0.26				
W28F, Oxidized	$C\delta_1$-W31	8.09	0.014	0.59
20°C, pH 8	$C\epsilon_3$-W31	8.09	0.015	0.60
r_0 = 0.31				
W28F, Reduced	$C\delta_1$-W31	10.5	0.012	0.71
20°C, pH 6.5	$C\epsilon_3$-W31	10.5	0.017	0.70
r_0 = 0.26				
W28F, Reduced	$C\delta_1$-W31	8.89	0.009	0.61
20°C, pH 6.5	$C\epsilon_3$-W31	8.89	0.012	0.60
r_0 = 0.31				
W28F, Reduced	$C\delta_1$-W31	9.91	0.015	0.65
20°C, pH 8.0	$C\epsilon_3$-W31	9.91	0.015	0.61
r_0 = 0.26				
W28F, Reduced	$C\delta_1$-W31	8.43	0.012	0.57
20°C, pH 8.0	$C\epsilon_3$-W31	8.43	0.012	0.53
r_0 = 0.31				
W28F, Reduced	$C\delta_1$-W31	4.64	0.010	0.60
50°C, pH 6.5	$C\epsilon_3$-W31	4.64	0.007	0.68

approximately by

$$\Delta(LW) = (4/15\pi)\alpha\beta' S^2\tau_m[1 + 0.75/(1 + \omega_C^2\tau_m^2)], \quad (13)$$

where the symbols were defined with Eq. 9. The product $S^2\tau_m$ can be calculated from Eq. 13 from the $\Delta(LW)$ data by observing that the second term in the brackets on the right-hand-side of Eq. 13 is small compared with 1 (it has a maximum value of 0.11 for these data) and can be estimated for suitable τ_m values with only small effect (<10%) on the resulting $S^2\tau_m$. In Table 8, comparisons of $S^2\tau_m$ values obtained from $\Delta(LW)$ and from the parameters in Tables 4 and 5 are given. Generally, the agreement is good. Thus, although differential broadening data do not allow the motional parameters to be recovered independently, they do provide a corroboration of the results of the direct relaxation rate measurements.

TABLE 8 Differential broadening for WT-TRX at 125.7 MHz and pH 6.5

T	Nucleus	$\Delta(LW)$*	$S^2\tau_m$	$S^2\tau_m$ (calc)
°C		Hz	ns	ns
		Oxidized protein		
20	$C\delta_1$-W28	14.2	7.6	7.0
	$C\delta_1$-W31	16.7	9.0	7.1
25	$C\delta_1$-W28	12.2	6.5	7.5
	$C\delta_1$-W31	13.2	7.1	7.0
35	$C\delta_1$-W28	9.4	4.9	6.6
	$C\delta_1$-W31	9.6	5.1	5.9
50	$C\delta_1$-W28	8.8	4.6	4.8
	$C\delta_1$-W31	7.6	3.9	4.4
		Reduced protein		
20	$C\delta_1$-W28	15.8	8.5	7.3
	$C\epsilon_3$-W28	20.8	6.1	5.7
	$C\delta_1$-W31	14.2	7.6	6.6
	$C\epsilon_3$-W31	20.5	6.0	6.7
25	$C\delta_1$-W28	10.9	5.8	7.2
	$C\epsilon_3$-W28	22.5	6.6	6.8
	$C\delta_1$-W31	10.2	5.5	6.6
	$C\epsilon_3$-W31	20.6	6.0	6.6
35	$C\delta_1$-W28	10.6	5.6	6.1
	$C\epsilon_3$-W28	11.8	3.4	5.9
	$C\delta_1$-W31	10.5	5.5	5.6
	$C\epsilon_3$-W31	18.8	5.4	5.1
50	$C\delta_1$-W28	7.4	3.8	4.3
	$C\delta_1$-W31	5.1	2.6	4.2

* Missing entries are due to spectral overlap.

Time-resolved fluorescence anisotropy measurements were made on oxidized and reduced W28F and W31F at pH 8.0 and 20°C. The reducing effect of TECP (Burns et al. 1991) on both mutants was evidenced by a 2.3- and 4.7-fold increase in the steady-state fluorescence intensity of W28F and W31F, respectively. The fluorescence intensity decay of both proteins was complex requiring four lifetime components to adequately describe the data, and the final fits of the intensity and anisotropy decays yielded reduced chi-squared values in the range 1.2–1.5. An example of the time-resolved anisotropy decay of reduced W28F is shown in Fig. 6, and the results of the analysis of the time-resolved anisotropy measurements are presented in Table 9 in terms of the parameters given in Eq. 11. The recovered errors for r_o τ_m, S^2, and τ_e are ±5, ±15, ±15, and ±70%, respectively. The order parameter values obtained from these data are in good agreement with those given in Table 7. In particular, in the case of W31F, a single rotational correlation time characteristic of the overall molecular rotation adequately described the anisotropy decay with no advantage gained by adding a second exponential term. This is further indication that trp-28 in W31F lacks internal mobility (S^2 = 1). For trp-31 in

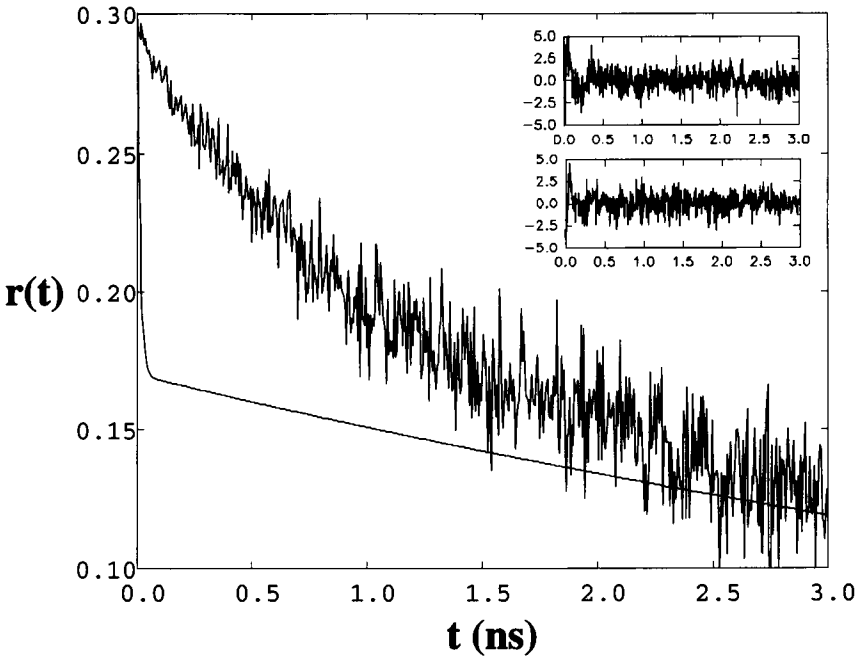

FIGURE 6 Time-resolved anisotropy decay $r(t)$ for trp-31 in reduced W28F at pH 8.0 and temperature 20°C derived from the experimental fluorescence decay data (*top* curve) and from the motional parameters obtained from NMR and given in Table 7 for $C\delta_1$-W31 (*bottom* curve). The NMR-derived $r(t)$ was scaled to have the same r_0 value as the fluorescence curve. The upper and lower insets correspond to the normalized residuals resulting from the fit shown in Table 9 vertically and horizontally polarized fluorescence emission respectively.

TABLE 9 Motional parameters obtained from tryptophan time-resolved anisotropy measurements of W31F and W28F at pH 8.0 and 20°C

Sample	r_0	τ_m	S^2	τ_e
		ns		ns
W31F, oxidized	0.28	5.5	1.0	—
W31F, reduced	0.30	5.4	1.0	—
W28F, oxidized	0.30	6.4	0.67	0.20
W28F, reduced	0.29	6.0	0.69	0.60

W28F, two rotational correlation times were required, which implies the presence of internal motion. A more detailed comparison of the findings of the different methodologies is included in the Discussion section.

DISCUSSION

The measured NOE values and the order parameters recovered from the analyses based upon the Lipari and Szabo (1982) formalism suggest strongly that the trp side chains in WT-TRX and W31F are nearly immobile, even at temperatures as high as 50°C. Some systematic, but small differences were observed. In oxidized WT-TRX at pH 6.5 and 20°C, the motion of trp-31 is perhaps slightly more restricted than that of trp-28. At other temperatures, and at pH 8.0 there was not a noticeable difference between the two residues. In reduced WT-TRX at pH 6.5, the motion of trp-31 is less restricted than that of trp-28 over the entire temperature range. Again at pH 8, there are no obvious differences, although the number of data are limited.

In the single trp variants, W28F and W31F, there were no significant differences in the trp side-chain motion between the oxidized and reduced proteins; however, a significant difference between the internal motion of trp-28 in W31F and trp-31 in W28F was observed in both oxidation states. The recovered order parameters for trp-31 were considerably smaller than those for trp-28, which themselves were quite similar to those obtained in the WT protein. Molecular modeling of W28F starting from the structure of WT-TRX obtained from NMR shows that trp-31 remains a surface residue as expected. Similarly, trp-28 in W31F remains partially buried. In the case of W28F, there must be subtle changes in the residues interacting with trp-31 that lead to the increased freedom of motion relative to that observed in WT-TRX.

The values found for τ_m from the analysis of the relaxation data are very consistent among the proteins for both oxidation states and at both pH values for a given temperature. There is no reason to expect a large change in protein volume upon reduction of the disulfide bond in TRX, but Kaminsky and Richards (1992) did find about a 5% decrease in the partial specific volume of reduced, as compared with oxidized, TRX. In all cases, our results were consistent with their finding. Larger τ_m values were obtained for the oxidized proteins, although the differences were normally less than the estimated uncertainties. Also, the good agreement of the $S^2\tau_m$ values found from the fits of the relaxation data with those calculated from the differential broadening data is gratifying. Further, the τ_m values obtained for WT-TRX at 35°C (Table 5) agree very well with those reported by Stone et al. (1993) (see below) from ^{15}N NMR relaxation measurements. These values are, however, somewhat larger than those estimated directly from the Stokes-Einstein equation, ~4–5 ns at 20°C (Cantor and Schimmel, 1980), based upon the molecular weight of the proteins, especially in the case of W28F and W31F at 20°C. τ_m values found from the anisotropy decay (Table 9) are in better agreement with the calculated values and are somewhat shorter than those derived from NMR. These points will be discussed further below. Fig. 7 does

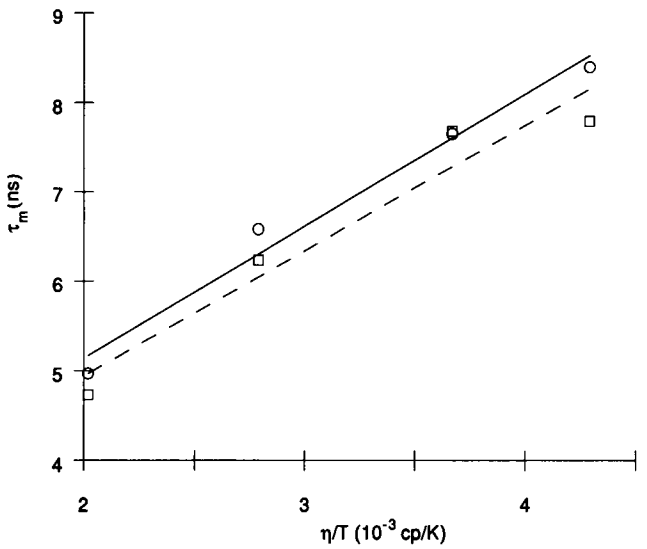

FIGURE 7 The overall correlation time τ_m versus the ratio of solution viscosity to temperature, η/T, for oxidized (○) and reduced (□) WT-TRX. Linear fits of the data are shown for the oxidized and reduced proteins by solid and dashed lines, respectively. The values of η for D_2O were calculated from Matsunaga and Nagashima (1983) using polynomial interpolation at temperatures for which η was not given.

demonstrate that for WT-TRX, τ_m obtained from the NMR relaxation data follows the predicted linear dependence on η/T, where η is the viscosity of the solution at a given (absolute) temperature, T.

As noted in Results, when T_2 was included in our analysis, even larger values were obtained for τ_m. For WT-TRX this amounts to only about a 5% increase in τ_m, whereas for W28F and W31F (results not shown), even at 50°C there is nearly a 100% increase in τ_m if T_2 is used leading to τ_m values, which are unphysical. Quantitative interpretation of T_2 in these sorts of dynamical measurements clearly must be treated with caution.

Stone et al. (1993) used NMR relaxation techniques to examine the dynamics of oxidized and reduced ^{15}N-labeled WT-TRX in solution at 35°C and pH 5.7. In addition to being isotopically labeled at the amide positions in the backbone, their samples also contained ^{15}N at the ϵ_1 (or 1) position of the indole rings of trp-28 and trp-31. As alluded to above, the agreement of τ_m values between our study and theirs was remarkable. Specifically, in the oxidized and reduced proteins at 35°C they report 6.41 and 6.31 ns, respectively, for τ_m to be compared with 6.58 and 6.24 ns found here. Similarly, they found the internal motion of the trp rings to be quite restricted. However, they found smaller order parameter values for trp-31 than for trp-28 in both the oxidized and reduced forms, whereas we only observed the difference between the two tryptophans in the reduced form. The numerical values for S^2 are in reasonable consonance, but our values are consistently larger, which could relate directly to either one, or both, of the observations that different vectors and different heteronuclei are being monitored in the two sets of experiments.

It is also possible to obtain order parameter values on the basis of Eq. 12 solely from the fluorescence lifetimes and steady-state anisotropy. Weaver et al. (1989) found that as a function of τ_e the order parameter derived form Eq. 12 has a step function behavior for a given τ_m. For $\tau_e \leq 500$ ps or so, which is the expected τ_e regime, S^2 approaches a limiting value. It is possible, therefore, to deduce values for S^2 for a chosen τ_m by taking the limit of Eq. 12 as $\tau_e \rightarrow 0$. As was the case with the combined NMR and fluorescence analysis, the result is strongly dependent on the value chosen for r_o. In Table 10 we compare the order parameter values obtained for W28F and W31F at 20°C and pH 6.5 by fluorescence alone with those found for $^{13}C\delta_1$-trp from the combined analysis for $r_o = 0.26$. To make the estimate of S^2 from the fluorescence data alone, a midrange value of τ_m based on the combined analysis (Table 7) of 9 ns was chosen. Overall, the results are quite consistent, although the errors in the analyses are inevitably large because of uncertainty in the appropriate r_o and because the experimental parameters, particularly the NOE, were often close to their theoretically limiting values.

Given order parameter values, it is possible to estimate the angular extent of the internal motion for specific models of the motion. In previous papers (Weaver et al., 1989, 1992), we applied a model in which the trp ring was considered to rotate as a unit about the β-γ bond only with all orientations equally probable within a restricted angular range of $\pm\phi_0$. In that model, the order parameter is given by

$$S^2 = 0.25(3\cos^2\theta_0 - 1)^2 + 3(\sin\theta_0\cos\theta_0\sin\phi_0/\phi_0)^2 + 0.1875(\sin^2\theta_0\sin 2\phi_0/\phi_0)^2, \quad (14)$$

where ϕ_0 is the fixed angle between the relevant C-H vector and the trp β-γ bond. From the coordinates of oxidized and reduced WT-TRX in the Protein Data Bank and schematically represented in Fig. 2, the values of ϕ_0 for $C\delta_1$-trp-28, and trp-31 are found to range from 71.6 to 73.5°, whereas those for $C\epsilon_3$-trp-28 and trp-31 range from 20.9 to 22°. If this motion were the only motion present, the order parameter value for $C\epsilon_3$-trp (S^2 (ϵ_3)) would be greater than that for $C\delta_1$-trp (S^2 (δ_1)) for the same ϕ_0 ($\neq 0$). For example, the minimum value that S^2 could have ($\phi_0 = 180°$) is 0.64 for $C\epsilon_3$-trp and 0.13 for $C\delta_1$-trp in this model. Because the $C\epsilon_3$-H vector makes a smaller angle with the β-γ bond, S^2 (ϵ_3) is less

TABLE 10 Comparison of order parameters obtained solely from fluorescence with those from the combined NMR and fluorescence analysis for $^{13}C\delta_1$-trp in W31F and W28F at 20°C with $r_o = 0.26$

Sample	S^2 Fluorescence only	S^2 Combined analysis
W31F, oxidized, pH 6.5	1.1	0.99
W31F, oxidized, pH 8.0	0.88	—
W31F, reduced, pH 6.5	1.0	0.94
W31F, reduced, pH 8.0	1.1	—
W28F, oxidized, pH 6.5	0.68	0.65
W28F, oxidized, pH 8.0	0.71	0.68
W28F, reduced, pH 6.5	0.73	0.71
W28F, reduced, pH 8.0	0.68	0.65

sensitive to rotation about that bond than is S^2 (δ_1). As seen from Tables 4–7, seldom did we find S^2 (ϵ_3) > S^2 (δ_1). In fact, generally for trp-28 in WT-TRX S^2 (ϵ_3) < S^2 (δ_1) (Tables 4 and 5). To the extent that differences among these intrinsically high order parameter values are reliable, they apparently indicate that the internal motion of the trp residues is more complex than just rotation about the β-γ bond, which is of course what would be expected a priori. Furthermore, in that regard, the protein coordinates reveal that the angle between the Cϵ_3-H vector and the α-β bond is ~80° and that between the Cδ_1-H vector and the α-β bond is ~52° for trp-28 in WT-TRX. Thus, rotation about the α-β bond should result in a larger reduction in S^2 (ϵ_3) than in S^2 (δ_1) for trp-28, which is consistent with the results. For trp-31, the difference between the angles that the two C-H vectors make with the α-β bond is smaller and the sense is reversed leading to the expectation of a smaller difference between S^2 (ϵ_3) and S^2 (δ_1), which is again consistent with the results.

In lieu of an appropriate, more complete model of the motion we can, nonetheless, use the above expression for S^2 to calculate corresponding values of ϕ_0. For the experimental conditions here, ϕ_0 ranges from 0 to 25° for the Cδ_1-H vector and 0 to 110° for the Cϵ_3-H vector for trp-28 and 31 in WT-TRX, from 6–26° for trp-28 in W31F and 40–47° for trp-31 in W28F for the Cδ_1-H vector, and from 58 to 97° for trp-28 in W31F and 115 to 180° for trp-31 in W28F for the Cϵ_3-H vector. Alternatively, if the Kinosita model (Kinosita et al., 1977) for motion of the vectors restricted within a cone of half-angle θ is used to interpret the order parameters, θ varies from 0 to 35° over the full range of the experiments.

From an experimental standpoint, the fundamental approach we have used here seems ideal for study of aromatic ring motions. Obviously, questions remain regarding a physical interpretation. We are hard put to give credence to small changes in S^2 in terms of presumed changes in amplitude of motion due to the uncertainties in the analysis, or to estimate actual amplitudes of angles of rotation for motion of the trp rings. However, despite the shortcomings given the trends seen for the S^2 parameters, hope remains that reasonable insight may be gained from even these order parameters regarding amplitude of motion, especially for comparison with inferences drawn from MD simulations or from minimum perturbation mapping calculations (Haydock, 1993).

The instability of the τ_e values is a disappointment. For TRX, τ_e fell in the range from 0 to about 3 ns, with the majority of the values being less than 60 ps. However, from the form of the spectral density, Eq. 8, it can be seen that when S^2 values are near 1, the τ_e values obtained are not likely to be well defined unless $\omega^2\tau_m \gg 1$. Only in the case of trp-31 in W28F, where the order parameters were smaller, can confidence be placed in the τ_e values. Those values were mostly in the range of 10–20 ps from NMR (Table 7) with a statistical uncertainty of about ±25% based on the goodness of the fit and uncertainties in the data. These τ_e are on the time scale expected, but the uncertainties are too large to allow differences present between the trp residues or the labeled positions to be interpreted with any confidence. Moreover, the τ_e values are considerably smaller than those obtained from the measurements of the time-resolved fluorescence anisotropy decay (Table 9) as seen directly for the example shown in Fig. 6, and they differ from the fluorescence values by amounts greater than the estimated uncertainties. Differences of a similar nature have been observed in work on peptides (P. Buckley, private communication), and their origins are being investigated. Here in a few instances, τ_e values on the nanosecond scale were found from the NMR measurements. This could indicate a failure in the spectral density of Eq. 8 to describe adequately our system (Clore et al., 1990a), and more data would be needed to resolve that question. Clearly, in general it is best to have NMR relaxation data at more than one frequency and/or to have steady-state anisotropy data available especially given the apparent lack of utility of T_2 values. Although the use of (NOE − 1)/T_1 in our data analysis did not in the end leave us with τ_e values in which we have a large degree of confidence, it did have the benefit of consistently yielding parameters that reproduced the experimental data better than those obtained using the NOE instead.

Our fluorescence steady-state anisotropy and decay data for W28F and W31F corroborate the NMR data well, particularly with regard to the order parameters. In W31F we were unable to recover evidence for subnanosecond motions. This implies, at least as far as the fluorescence data are concerned, that any depolarization of the fluorescence signal evident in an $r_0 < 0.4$ recovered by extrapolation of the $r(t)$ curve to $t = 0$ is due to other factors. Either there are local motions too fast to be detected by our instrumentation or there are electronic effects on the fundamental photophysics of the indole moiety that we do not know, frankly, and we cannot even speculate about at this point. We prefer the former explanation.

Earlier measurements of tryptophan fluorescence anisotropy decay in TRX were reported by two groups. Our NMR results for trp-31 agree generally with the inferences drawn by Mérola et al. (1989), who deduced the existence of very fast (subnanosecond) trp internal motions in reduced as compared with oxidized WT-TRX. These comparisons are clouded, however, by the observation that interpretation of anisotropy decay data when there are two emitters is, at best, very difficult particularly when the overall quantum yield is as low as it is in TRX. Furthermore, the parameters of motion are unavoidably derived from a fitting procedure and therefore carry with them, intrinsically, no physical meaning. It is the investigator who imparts a physical interpretation. This can be done credibly only if the numbers can be shown to be altered predictably by some perturbation such as temperature change or if the derived parameters can be corroborated by data gathered with another spectroscopic technique. Accordingly, we do not find it justifiable at this juncture to draw any inferences from our results regarding the rate of ring libration for the trp rings in WT-TRX, but are convinced that both trp-31 and trp-28 are quite rigidly held, the latter more so than the former. The second group, Elofsson et al. (1991), concluded that the internal mobility of trp-28 in WT-TRX was

quite restricted in agreement with our results. In addition, they examined the mutant W31F and found increased motion of trp-28 relative to the WT protein which was not indicated in our measurements. The origin of differences in the results for W31F is not apparent. It is worth noting however that Elofsson et al. (1991) also gave results of MD simulations on WT-TRX which are in general agreement with our NMR measurements in that the motion of trp-28 was quite restricted and showed little change between the oxidized and the reduced protein whereas the motion of trp-31 was restricted in the oxidized protein, but showed an increase in motion upon reduction of the protein. Additional MD simulations on WT-TRX by Elofsson and Nilsson (1993) similarly indicated trp-28 to be very restricted and trp-31 to be only slightly more free to move in the oxidized protein, whereas each residue showed a slight increase in mobility in the reduced protein.

The τ_m values reported by Mérola et al. (1989) and Elofsson et al. (1991) tended to be somewhat lower than the values found here from NMR, but reasonably consistent with our time-resolved anisotropy results. The difference in τ_m values obtained from NMR and fluorescence is a source for continuing investigation. Similar observations were made by Palmer et al. (1993) for a zinc-finger peptide and by Chazin (private communication) for calbindin D_{9k}. It has been observed that TRX has a tendency to form dimers at pH values $\leq$5.5 (Holmgren, 1985). For that reason our samples were maintained at pH 6.5 and 8.0, and also experiments were done at temperatures up to 50°C. There were no obvious indications of dimerization from the NMR spectra, but the NMR measurements were made at approximately 20 times the concentration of the fluorescence measurements due to experimental constraints, and the differences in τ_m values observed between NMR and fluorescence may be related ultimately to the differences in sample concentrations and concomitant hydration or excluded volume effects, or to other yet to be recognized details of data interpretation.

Finally, is there a clear structural basis for the immobilization of the aromatic rings in TRX? An examination of the structure derived from x-ray crystallography of oxidized TRX (Holmgren et al., 1975; Katti et al., 1990) (Fig. 1) (the x-ray structure of reduced TRX is not available) shows that the indole ring of trp-28 is tightly packed into the protein matrix as noted above and presumably quite rigidly held, consistent with our results. Of particular relevance is that this inference is fully substantiated by the solution structure derived from multidimensional NMR data for oxidized and reduced TRX (Dyson et al., 1990). By comparison, the situation regarding trp-31 is somewhat more intriguing. Given its location at the surface of TRX, at least one face of the ring of trp-31 is fully accessible to solvent. In particular, Connolly solvent accessibility calculations (M. L. Connolly, unpublished results) of trp-28 and trp-31 verify that, indeed, trp-31 is more exposed. Using CHARMM and Quanta software (Molecular Simulations, Inc., Burlington, MA), we added all of the hydrogen atoms to the x-ray structure of oxidized TRX and then calculated the solvent-accessible area for trp-31 to be 106 Å^2 and that for trp-28 to be 51 Å^2 for a probe radius of 1.4 Å. One is tempted to infer, a priori, that the trp-31 indole ring would be quite mobile. However, the x-ray crystallographic data yield Debye-Waller (B) factors consistent with a highly resolved, relatively immobile ring (Holmgren et al., 1975; Katti et al., 1990). The orientation of the ring, lying essentially flat on a surface, and low B factors suggest substantial nonbonded interactions with the protein matrix. For librations (or rotations) of substantial magnitude to occur, the indole ring would first have to lift off the surface. Minimum perturbation mapping calculations (N. Silva, C. Haydock, and F. G. Prendergast, unpublished data) suggest that it is feasible for trp-31 to lift from the surface, but that it would probably not happen on the picosecond to nanosecond time scale given the apparent energetic barriers. Interestingly, such surface locations for trp rings are relatively common, for example, trp-15 in liver alcohol dehydrogenase (Eftink and Ghiron, 1977; Ross et al., 1981), trp-140 in *Staph.* nuclease (Eftink et al. 1989), and trp-3 in porcine pancreatic phospholipase A_2 (Ludescher et al., 1985). In all three of these proteins, the dominant fluorescence lifetime is relatively long, and the fluorescence anisotropy data suggest that the trp side chain is almost irrotational. These results indicate that effects of the protein matrix on the tryptophan photophysics and dynamics are consonant with nonbonded interactions of the indole ring (H. V. Jakubowski and F. G. Prendergast, unpublished data; Axelsen and Prendergast, 1989; Axelsen et al., 1991).

Despite the difficulties encountered with the measurements reported here on TRX, we are convinced of the value of the two-pronged spectroscopic approach to the study of fluorophore motion (Weaver et al., 1988, 1989, 1992; Kemple et al., 1993; Palmer et al., 1993) as distinct from the analysis of possible rotamer populations. We need to find, however, proteins in which the trp (or tyr) rings are much freer to move than they are in TRX so that we may not only validate the methods but also actually *measure* amplitudes and rates of motion confidently, and subsequently compare them with trajectories from MD simulations. To date, little attention has been paid to τ_e. It remains to be verified to what extent values obtained so far for τ_e reflect physical reality. Interestingly, it is our experience so far that in many wild-type proteins the indole side chain of trp is either "buried," i.e., "tightly" packed, in the protein matrix *or* that the indole ring lies on the protein surface and is immobilized by nonbonding interactions at the surface as noted above. In the latter instance, the ring exhibits only collective motions, i.e., either segmental mobility or whole protein rotation. Insertion of trp residues into unnatural locations in proteins by recombinant DNA techniques offers more hope of finding a model system.

We would like to acknowledge the help of Drs. N. Murali and B. D. Ray of the IUPUI NMR Center.

This work was supported in part by National Science Foundation Grant DMB-9105885 to M. D. Kemple and by Public Health Service Grant GM34847 to F. G. Prendergast.

REFERENCES

Abragam, A. 1961. Principles of Nuclear Magnetism. Clarendon Press, Oxford. Ch. VIII.

Axelsen, P. H., E. Gratton, and F. G. Prendergast. 1991. Experimentally verifying molecular dynamics simulations through fluorescence anisotropy measurements. *Biochemistry*. 30:1173–1179.

Axelsen, P. H., and F. G. Prendergast. 1989. Molecular dynamics of tryptophan in ribonuclease-T1. II. Correlations with fluorescence. *Biophys. J.* 56:43–66.

Barbato, G., M. Ikura, L. E. Kay, R. W. Pastor, and A. Bax. 1992. Backbone dynamics of calmodulin studied by ^{15}N relaxation using inverse detected two-dimensional NMR spectroscopy: the central helix is flexible. *Biochemistry*. 31:5269–5278.

Beechem, J. M., and E. Gratton. 1988. Fluorescence spectroscopy data analysis environment: a second generation global analysis program. *Proc. S.P.I.E.* 909:70–81.

Boyd, J., U. Hommel, and I. D. Campbell. 1990. Influence of cross-correlation between dipolar and anisotropic chemical shift relaxation mechanisms upon longitudinal relaxation rates of ^{15}N in macromolecules. *Chem. Phys. Lett.* 175:477–482.

Brooks III, C. L., M. Karplus, and B. M. Pettitt. 1988. Proteins: A Theoretical Perspective of Dynamics, Structure, and Thermodynamics. John Wiley & Sons, New York. 259 pp.

Burns, J. A., J. C. Butler, J. Moran, and G. W. Whitesides. 1991. Selective reduction of disulfides by tris(2-carboxyethyl)phosphine. *J. Org. Chem.* 56:2648–2650.

Cantor, C. R., and P. R. Schimmel. 1980. Biophysical Chemistry, Part II. W. H. Freeman, San Francisco, CA. Chapter 10.

Cheng, J.-W., C. A. Lepre, S. P. Chambers, J. R. Fulghum, J. A. Thomson, and J. M. Moore. 1993. ^{15}N NMR relaxation studies of the FK506 binding protein: backbone dynamics of the uncomplexed receptor. *Biochemistry*. 32:9000–9010.

Clore, G. M., A. Szabo, A. Bax, L. E. Kay, P. C. Driscoll, and A. M. Gronenborn. 1990a. Deviations from the simple two-parameter model-free approach to the interpretation of nitrogen-15 nuclear magnetic relaxation of proteins. *J. Amer. Chem. Soc.* 112:4989–4991.

Clore, G. M., P. C. Driscoll, P. T. Wingfield, and A. M. Gronenborn. 1990b. Analysis of the backbone dynamics of interleukin-1β using two-dimensional inverse detected heteronuclear ^{15}N-^{1}H NMR spectroscopy. *Biochemistry*. 29:7387–7401.

Dellwo, M. J., and A. J. Wand. 1989. Model-independent and model-dependent analysis of the global and intenal dynamics of cyclosporin A. *J. Amer. Chem. Soc.* 111:4571–4578.

Drapeau, G. R., W. J. Brammer, and C. Yanofsky. 1968. Amino acid replacements of the glutamic acid residue at position 48 in the tryptophan synthetase A protein of *Escherichia coli*. *J. Mol. Biol.* 35:357–367.

Dyson, H. J., G. P. Gippert, D. A. Case, A. Holmgren, and P. E. Wright. 1990. Three-dimensional solution structure of the reduced form of *Escherchia coli* thioredoxin determined by nuclear magnetic resonance spectroscopy. *Biochemistry*. 29:4129–4136.

Dyson, H. J., A. Holmgren, and P. E. Wright. 1989. Assignment of the proton NMR spectrum of reduced and oxidized thioredoxin: sequence-specific assignments, secondary structure, and global fold. *Biochemistry*. 28:7074–7087.

Eftink, M. R., and C. A. Ghiron. 1977. Exposure of tryptophanyl residues and protein dynamics. *Biochemistry*. 16:5546–5551.

Eftink, M. R., C. A. Ghiron, R. A. Kautz, and R. O. Fox. 1989. Fluorescence lifetime studies with staphylococcal nuclease and its site-directed mutant. Test of the hypothesis that proline isomerism is the basis for nonexponential decays. *Biophys. J.* 55:575–579.

Elbayed, K., and D. Canet. 1989. Accurate determination of interference terms between carbon-proton dipolar interactions and carbon or proton chemical shift anisotropy from longitudinal carbon-13 relaxation studies. *Mol. Phys.* 68:1033–1046.

Elofsson, A., and L. Nilsson. 1993. How consistent are molecular dynamics simulations? Comparing structure and dynamics in reduced and oxidized *Escherichia coli* thioredoxin. *J. Mol. Biol.* 233:766–780.

Elofsson, A., R. Rigler, L. Nilsson, J. Roslund, G. Krause, and A. Holmgren. 1991. Motion of aromatic side chains, picosecond fluorescence, and internal energy transfer in *Escherichia coli* thioredoxin studied by site-directed mutagenesis, time-resolved fluorescence spectroscopy, and molecular dynamics simulations. *Biochemistry*. 30:9648–9656.

Goldman, M. 1984. Interference effects in the relaxation of a pair of unlike spin-1/2 nuclei. *J. Magn. Reson.* 60:437–452.

Haydock, C. 1993. Protein side chain rotational isomerization: a minimum perturbation mapping study. *J. Chem. Phys.* 98:8199–8214.

Holmgren, A. 1972. Tryptophan fluorescence study of conformational transitions of the oxidized and reduced forms of thioredoxin. *J. Biol. Chem.* 247:1992–1998.

Holmgren, A. 1985. Thioredoxin. *Annu. Rev. Biochem.* 54:237–271.

Holmgren, A. 1989. Thioredoxin and glutaredoxin systems. *J. Biol. Chem.* 264:13963–13966.

Holmgren, A., and B.-M. Sjöberg. 1972. Immunochemistry of thioredoxin I. Preparation and cross-reactivity of antibodies against thioredoxin from *Escherichia coli* and bacteriophage T4. *J. Biol. Chem.* 247:4160–4164.

Holmgren, A., B.-O. Söderberg, H. Eklund, and C.-I. Bränden. 1975. Three-dimensional structure of *Escherichia coli* thioredoxin-S_2 to 2.8-Å resolution. *Proc. Natl. Acad. Sci. USA*. 72:2305–2309.

Kaminsky, S. M., and F. M. Richards. 1992. Reduction of thioredoxin significantly decreases its partial specific volume and adiabatic compressibility. *Protein Sci.* 1:22–30.

Katti, S. K., D. M. LeMaster, and H. Eklund. 1990. Crystal structure of thioredoxin from *Escherichia coli* at 1.68 Å resolution. *J. Mol. Biol.* 212:167–184.

Kay, L. E., L. K. Nicholoson, F. Delaglio, A. Bax, and D. A. Torchia. 1992. Pulse sequences for removal of the effects of cross correlation between dipolar and chemical-shift anisotropy relaxation mechanisms on the measurement of heteronuclear T_1 and T_2 values in proteins. *J. Magn. Reson.* 97:359–375.

Kemple, M. D., K. E. Nollet, P. Yuan, and F. G. Prendergast. 1993. "Active-site" dynamics: a comparison of the wild type and single tryptophan variants of *E. coli* thioredoxin. *In* Techniques in Protein Chemistry IV. R. H. Angeletti, editor. Academic Press, New York. 595–603.

Kinosita, K., S. Kawato, and A. Ikegami. 1977. A theory of fluorescence polarization decay in membranes. *Biophys. J.* 20:289–305.

Kunkel, T. A. 1985. Rapid and efficient site-specific mutagenesis without phenotypic selection. *Proc. Natl. Acad. Sci. USA*. 82:488–492.

Lakowicz, J. R., B. P. Maliwal, H. Cherek, and A. Balter. 1983. Rotational freedom of tryptophan residues in proteins and peptides. *Biochemistry*. 22:1741–1752.

Langsetmo, K., J. Fuchs, and C. Woodward. 1989. *Escherichia coli* thioredoxin folds into two compact forms of different stability to urea denaturation. *Biochemistry*. 28:3211–3220.

LeMaster, D. M., and F. M. Richards. 1988. NMR sequential assignment of *Escherichia coli* thioredoxin utilizing random fractional deuteration. *Biochemistry*. 27:142–150.

Lipari, G., and A. Szabo. 1982. Model-free approach to the interpretation of nuclear magnetic resonance relaxation in macromolecules. 1. Theory and range of validity. *J. Amer. Chem. Soc.* 104:4546–4559.

Ludescher, R. D., J. J. Volwerk, G. H. de Haas, and B. S. Hudson. 1985. Complex photophysics of the single tryptophan of porcine pancreatic phospolipase A_2, its zymogen, and an enzyme/micelle complex. *Biochemistry*. 24:7240–7249.

Matsunaga, N., and A. Nagashima. 1983. Transport properties of liquid and gaseous D_2O over a wide range of temperature and pressure. *J. Phys. Chem. Ref. Data*. 12:933–966.

Matthews, S. J., S. K. Jandu, and R. L. Leatherbarrow. 1993. ^{13}C NMR study of the effects of mutation on the tryptophan dynamics in chymotrypsin inhibitor 2: correlations with structure and stability. *Biochemistry*. 32: 657–662.

McCammon, J. A., and S. Harvey. 1987. Dynamics of Proteins and Nucleic Acids. Cambridge University Press, Cambridge. 234 pp.

Meiboom, S., and D. Gill. 1958. Modified spin-echo method for measuring nuclear relaxation times. *Rev. Sci. Instr.* 29:688–691.

Mérola, F., R. Rigler, A. Holmgren, and J.-C. Brochon. 1989. Picosecond tryptophan fluorescence of thioredoxin: evidence for discrete species in slow exchange. *Biochemistry*. 28:3383–3398.

Nageswara Rao, B. D., and B. D. Ray. 1992. ^{13}C NMR line shapes of [2-^{13}C]ATP in enzyme complexes and viscous solutions: glycosidic rotation persists at high viscosities and is arrested in enzyme complexes. *J. Amer. Chem. Soc.* 114:1566–1573.

Palmer III, A. G., R. A. Hochstrasser, D. P. Millar, M. Rance, and P. E. Wright. 1993. Characterization of amino acid side chain dynamics in a zinc-finger peptide using ^{13}C NMR spectroscopy and time-resolved fluorescence spectroscopy. *J. Amer. Chem. Soc.* 115:6333–6345.

Palmer III, A., G., M. Rance, and P. E. Wright. 1991. Intramolecular motions of a zinc finger DNA-binding domain from Xfin characterized by proton-detected natural abundance ^{13}C heteronuclear NMR spectroscopy. *J. Amer. Chem. Soc.* 113:4371–4380.

Palmer III, A. G., N. J. Skelton, W. J. Chazin, P. E. Wright, and M. Rance. 1992. Suppression of the effects of cross-correlation between dipolar and anisotropic chemical shift relaxation mechanisms in the measurement of spin-spin relaxation rates. *Mol. Phys.* 75:699–711.

Peng, J. W., V. Thanabal, and G. Wagner. 1992. Improved accuracy of heteronuclear relaxation time measurements in macromolecules. Elimination of anti-phase contributions. *J. Magn. Reson.* 95:421–427.

Peng, J. W., and G. Wagner. 1992. Mapping of the spectral densities of N-H bond motions in eglin c using heteronuclear relaxation experiments. *Biochemistry.* 31:8571–8586.

Piatini, U., O. W. Sørensen, and R. R. Ernst. 1982. Multiple quantum filters for elucidating NMR coupling networks. *J. Amer. Chem. Soc.* 104: 6800–6801.

Rance, M., O. W. Sørensen, G. Bodenhausen, G. Wagner, R. R. Ernst, K. Wüthrich. 1983. Improved spectral resolution in COSY ^{1}H NMR spectra of proteins via double quantum filtering. *Biochem. Biophys. Res. Commun.* 117:479–485.

Redfield, C., J. Boyd, L. J. Smith, R. A. G. Smith, and C. M. Dobson. 1992. Loop mobility in a four-helix-bundle protein: ^{15}N NMR relaxation measurements on human interleukin-4. *Biochemistry.* 31:10431–10437.

Reutimann, H., B. Straub, P. L. Luisi, and A. Holmgren. 1981. A conformational study of thioredoxin and its tryptic fragments. *J. Biol. Chem.* 256:6796–6803.

Ross, J. B. A., C. J. Schmidt, and L. Brand. 1981. Time-resolved fluorescence of the two tryptophans in horse liver alcohol dehydrogenase. *Biochemistry.* 20:4369–4377.

Ruggiero, A. J., D. C. Todd, and G. R. Fleming. 1990. Subpicosecond fluorescence anisotropy studies of tryptophan in water. *J. Amer. Chem. Soc.* 112:1003–1014.

Schneider, D. M., M. J. Dellwo, and A. J. Wand. 1992. Fast internal main-chain dynamics of human ubiquitin. *Biochemistry.* 31:3645–3652.

Separovic, F., K. Hayamizu, R. Smith, and B. A. Cornell. 1991. C-13 chemical shift tensor of L-tryptophan and its application to polypeptide structure determination. *Chem. Phys. Lett.* 181:157–162.

Shaka, A. J., J. Keeler, and R. Freeman. 1983. Evaluation of a new broadband decoupling sequence: Waltz-16. *J. Magn. Reson.* 53:313–340.

Stone, M. J., K. Chandrasekhar, A. Holmgren, P. E. Wright, and H. J. Dyson. 1993. Comparison of backbone and tryptophan side-chain dynamics of reduced and oxidized *Escherichia coli* thioredoxin using ^{15}N NMR relaxation measurements. *Biochemistry.* 32:426–435.

Summers, M. F., L. G. Marzilli, and A. Bax. 1986. Complete ^{1}H and ^{13}C assignments of coenzyme B_{12} through the use of new two-dimensional NMR experiments. 1986. *J. Amer. Chem. Soc.* 108:4285–4294.

Valeur, B., and G. Weber. 1977. Resolution of the fluorescence excitation spectrum of indole into the $^{1}L_a$ and $^{1}L_b$ excitation bands. *Photochem. Photobiol.* 25:441–444.

Weaver, A. J., M. D. Kemple, J. W. Brauner, R. Mendelsohn, and F. G. Prendergast. 1992. Fluorescence, CD, attenuated total reflectance (ATR) FTIR, and ^{13}C NMR characterization of the structure and dynamics of synthetic melittin and melittin analogues in lipid environments. *Biochemistry.* 31:1301–1313.

Weaver, A. J., M. D. Kemple, and F. G. Prendergast. 1988. Tryptophan sidechain dynamics in hydrophobic oligopeptides determined by use of ^{13}C nuclear magnetic resonance spectroscopy. *Biophys. J.* 54:1–15.

Weaver, A. J., M. D. Kemple, and F. G. Prendergast. 1989. Fluorescence and ^{13}C NMR determination of side-chain and backbone dynamics of synthetic melittin and melittin analogues in isotropic solvents. *Biochemistry.* 28:8624–8639.